This is an open access article published under an ACS AuthorChoice License, which permits copying and redistribution of the article or any adaptations for non-commercial purposes.

Journal of Medicinal Chemistry

Article

pubs.acs.org/jmc

Simplified 2-Aminoquinoline-Based Scaffold for Potent and Selective Neuronal Nitric Oxide Synthase Inhibition

Maris A. Cinelli,[†] Huiying Li,[‡] Georges Chreifi,[‡] Pavel Martásek,[§,∥] Linda J. Roman,[§] Thomas L. Poulos,*[,‡] and Richard B. Silverman*[,†]

[†]Departments of Chemistry and Molecular Biosciences, Chemistry of Life Processes Institute, Center for Molecular Innovation and Drug Discovery, Northwestern University, 2145 Sheridan Road, Evanston, Illinois 60208-3113, United States

[‡]Departments of Molecular Biology and Biochemistry, Pharmaceutical Sciences, and Chemistry, University of California, Irvine, California 92697-3900, United States

[§]Department of Biochemistry, University of Texas Health Science Center, San Antonio, Texas 78384-7760, United States

[∥]Department of Pediatrics and Center for Applied Genomics, First School of Medicine, Charles University, Prague, Czech Republic

Supporting Information

ABSTRACT: Since high levels of nitric oxide (NO) are implicated in neurodegenerative disorders, inhibition of the neuronal isoform of nitric oxide synthase (nNOS) and reduction of NO levels are therapeutically desirable. Nonetheless, many nNOS inhibitors mimic L-arginine and are poorly bioavailable. 2-Aminoquinoline-based scaffolds were designed with the hope that they could (a) mimic aminopyridines as potent, isoform-selective arginine isosteres and (b) possess chemical properties more conducive to oral bioavailability and CNS penetration. A series of these compounds was synthesized and assayed against purified nNOS enzymes, endothelial NOS (eNOS), and inducible NOS (iNOS). Several compounds built on a 7-substituted 2-aminoquinoline core are potent and isoform-selective; X-ray crystallography indicates that aminoquinolines exert inhibitory effects by mimicking substrate interactions with the conserved active site glutamate residue. The most potent and selective compounds, **7** and **15**, were tested in a Caco-2 assay and showed good permeability and low efflux, suggesting high potential for oral bioavailability.

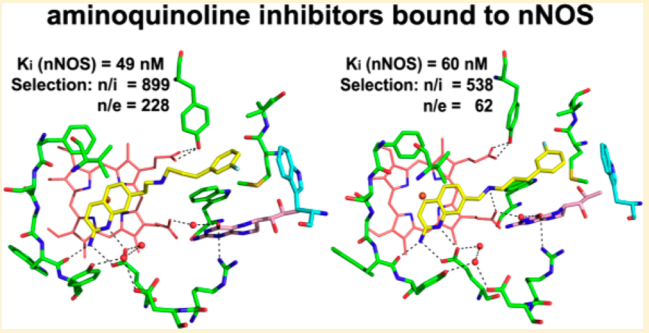

INTRODUCTION

The term *neurodenegerative disorder* is used to describe diseases characterized by the progressive breakdown of neuronal function and structure. This term encompasses disorders such as Alzheimer's, Parkinson's, and Huntington's diseases, as well as amyotrophic lateral sclerosis (ALS), among others, although neuronal damage is also associated with stroke and ischemic events, cerebral palsy, and head trauma. Although the human and economic cost of neurodegeneration continues to be astronomical, treatment is largely limited to palliative care and prevention of symptom progression. Therefore, there is a constant demand for novel and effective approaches to slow or prevent the progression of these diseases.

One target under investigation is neuronal nitric oxide synthase (nNOS). Nitric oxide (NO) is an important second messenger in the human body, and dysregulation of its production is implicated in many pathologies. NO is produced by the nitric oxide synthase enzymes, of which there are three isoforms: endothelial nitric oxide synthase (eNOS), which regulates blood pressure and flow, inducible nitric oxide synthase (iNOS), involved in immune system activation, and nNOS, which is required for normal neuronal signaling.[1] Nonetheless, overexpression of nNOS in neural tissue and increased levels of NO can result in protein nitration and oxidative damage to neurons, especially if peroxynitrite is formed from excess NO.[2,3] Indeed, overexpression of nNOS or excess NO has been implicated in or associated with many neurodegenerative disorders.[4−10] The inhibition of nNOS is, therefore, a viable therapeutic strategy for preventing or treating neuronal damage.[11−13]

All NOS enzymes are active only as homodimers. Each monomer consists of both a reductase domain with FAD, FMN, and NADPH binding sites, and a heme-containing oxygenase domain, where the substrate (L-arginine) and cofactor (6*R*)-5,6,7,8-tetrahydrobiopterin (H_4B) bind. Activated and regulated by calmodulin binding, electron flow proceeds from one monomer's reductase domain to the other's oxygenase domain,[14] catalyzing the oxidation of arginine to citrulline with concomitant production of NO.[15]

Not unexpectedly, most investigated nNOS inhibitors are mimetics of arginine and act as competitive inhibitors. One

Received: November 27, 2013
Published: January 28, 2014

 © 2014 American Chemical Society dx.doi.org/10.1021/jm401838x | J. Med. Chem. 2014, 57, 1513−1530

major challenge in designing nNOS inhibitors is that eNOS and iNOS share high sequence similarity and an identical overall architecture with nNOS,[13,16] especially in their substrate-binding sites. Lack of isoform selectivity could have deleterious effects; inhibition of eNOS can cause severe hypertension, and iNOS inhibition could impair immune system activation. Previously, in our laboratories, fragment hopping[17] and subsequent structure-based optimization[18] afforded compounds **1** and **2** (representative nNOS inhibitors are shown in Figure 1). These compounds are highly potent and selective nNOS

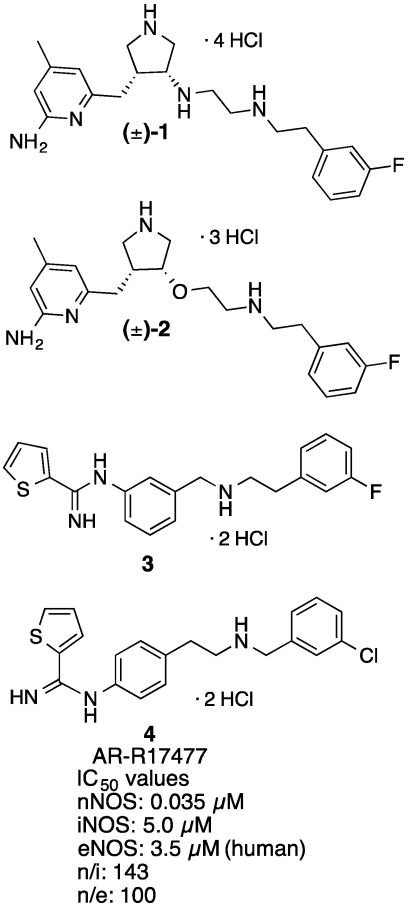

Figure 1. Representative nNOS inhibitors discussed in this study.

inhibitors, and compound **1** reverses a hypoxic-ischemic brain damage phenotype in newborn rabbit kits when administered intravenously to the dam.[19]

Although effective, compounds **1** and **2** suffer from several drawbacks. Like most arginine mimics, they are very polar and hydrophilic and contain numerous basic moieties and hydrogen-bond donors, as well as many rotatable bonds and a high total polar surface area (tPSA), all properties that hamper both GI absorption and blood–brain barrier permeation.[20,21] Many attempts to improve the bioavailability of these compounds have been made, including alkylation,[22] fluorination,[23] introduction of lipophilic tails,[24] and replacement of the amines;[25] most of these strategies either diminished potency or selectivity or were synthetically challenging. The chiral scaffolds of **1** and **2** are also difficult (>12 steps) to prepare, making them less desirable than simpler scaffolds, such as **3**[26] and the AstraZeneca candidate **4** (AR-R17477; potencies and selectivities are given in Figure 1[27]) from a clinical standpoint. Nonetheless, these simplified molecules are not without fault; their isoform selectivities are lower, **3** suffers from poor Caco-2 permeability, and **4** is much less potent in cell-based assays[28] than against isolated enzymes, both likely the result, in part, of the amidine moiety, which will be charged at physiological pH.

One avenue that we wished to explore for the generation of simpler nNOS inhibitor scaffolds was the replacement of the amidine group of a molecule such as **3** with another arginine isostere. Such a group should be stable, weakly basic (pK_a between 6 and 8), and possess as few hydrogen-bond donors as possible. One such moiety is the 2-aminoquinoline group (pK_a of 7.3[29]), which is desirable because of both its resemblance to the aminopyridines of **1** and **2** (in both structure and pK_a, which is 7.1 for 2-aminopyridine[30]) and its considerably higher cLogP. We were also encouraged by the reported use of dihydroaminoquinolines as nNOS inhibitors by Jaroch et al.[31−33] Additionally, a recent report indicates that 2-aminoquinoline-based BACE-1 inhibitors have high cellular activity and good blood–brain barrier permeability in a rat model.[34] To this end, 2-aminoquinoline and the structure of **3** were effectively "hybridized" to produce compound **5**, a simple compound with good calculated physicochemical properties. We then proposed several other modifications to this scaffold (Figure 2). There is a hydrophobic pocket at the far end of the substrate access channel of nNOS; contact between an inhibitor and the residues lining this pocket is implicated in high selectivity for nNOS over the other two isoforms.[27,35] Preliminary docking studies and crystallography indicated that elongation of the chain between the aminoquinoline system and the distal fluorophenyl ring of **5**, moving the position of the secondary amine, or a combination of both, might provide the right length and orientation to reach this hydrophobic pocket, and a series of analogues investigating chain length (**6**–**9**) and nitrogen position was, therefore, prepared (Figure 2). Additionally, on the basis of computer modeling, we hypothesized that placement of the "tail" of the inhibitor at position 6 of the aminoquinoline system (instead of position 7) could also be effective; to this end, compounds **10**–**13** were prepared (Figure 2). Finally, several literature studies[17,36] indicate that the use of other halogens and substitution patterns on the noncoordinating aryl ring could be beneficial for enhancing potency and selectivity, so a small series of 7-substituted compounds (**14**–**16**) with different halogens and substitution patterns was prepared (Figure 2). All compounds were assayed against purified rat nNOS, and select compounds were assayed against eNOS, iNOS, and human nNOS, and for cellular permeability in a Caco-2 model.

CHEMISTRY

6- and 7-Substituted 2-aminoquinolines were prepared by methods originally reported by Manimaran et al.[37] and Johnson et al.[38] In the present study, 7-substituted aminoquinolines (**5**–**9** and **14**–**16**) were prepared by a versatile, late-divergent route that began with the preparation of 3′-methylcinnamanilide (**17**) by literature procedures.[39,40] Compound **17** was subsequently treated with an excess of aluminum chloride in chlorobenzene to affect cyclization and concomitant cleavage of the C-aryl bond to yield the carbostyril **18** as a mixture of the 7-isomer **18a** (major) and 5-isomer **18b** (minor).[39−41] The isomers were not separated at this stage but were converted into the 2-chloroquinolines **19a** and **19b**; the unwanted 5-isomer **19b** was removed by fractional crystallization.[41] Pure **19a** was converted into 2-acetamidoquinoline **20** by the method of Kóródi,[42] and

dx.doi.org/10.1021/jm401838x | J. Med. Chem. 2014, 57, 1513−1530

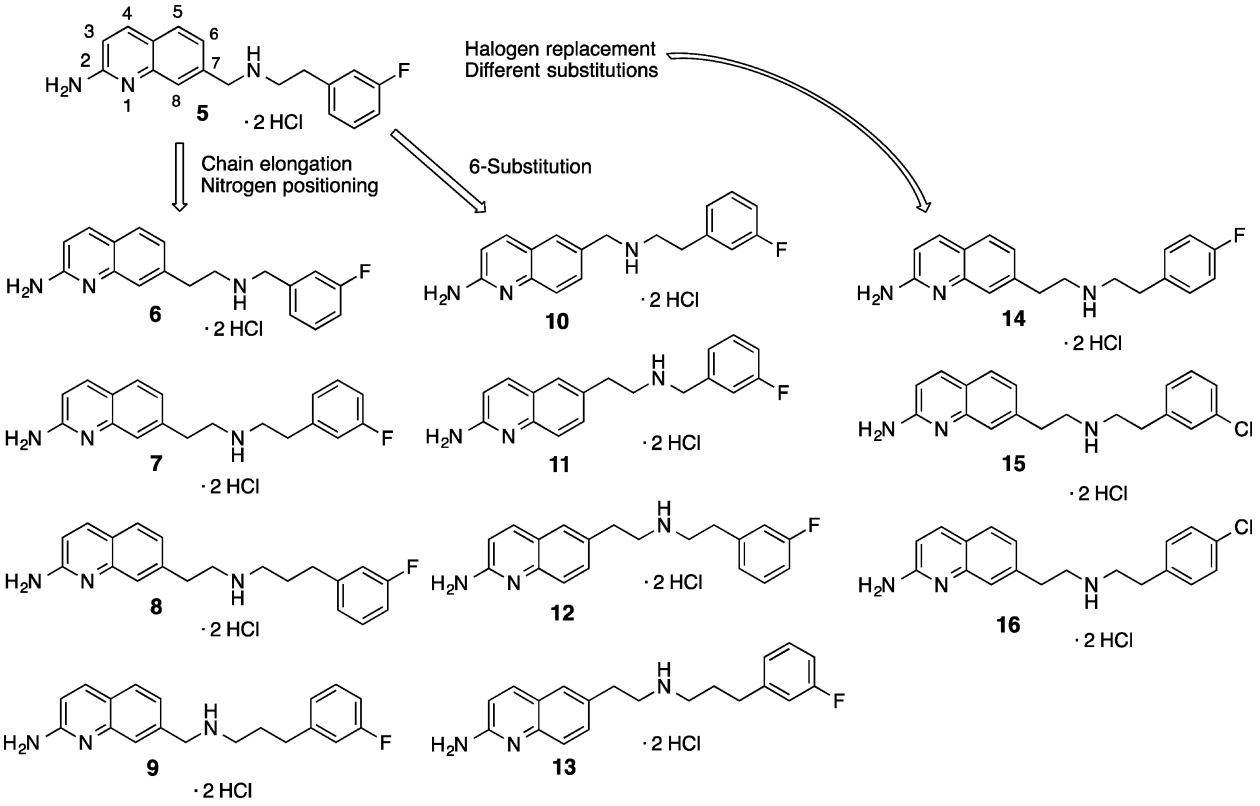

Figure 2. Inhibitor design strategy and 2-aminoquinolines synthesized in this study.

free-radical bromination[40] afforded versatile intermediate **21** (Scheme 1).

Scheme 1[a]

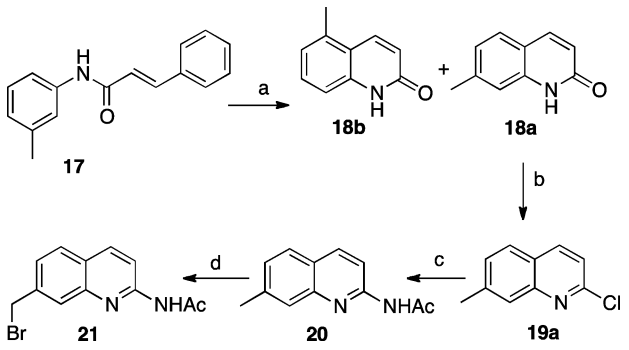

[a]Reagents and conditions: (a) $AlCl_3$, PhCl, 90 °C; (b) (i) $POCl_3$, reflux, (ii) fractional crystallization from *i*-PrOH after isolation; (c) $AcNH_2$ K_2CO_3, reflux (~230 °C); (d) NBS, $(PhCO_2)_2$, benzene, reflux.

To prepare aminoquinoline analogues with one methylene unit between the quinoline system and the secondary amine (**5** and **9**, Schemes 2 and 3), compound **21** was treated with 3-fluorophenethylamine (**22**, Scheme 2) or 3-fluoro-1-phenylpropanamine (**25**, Scheme 3, prepared by hydrogenation of 3-fluorophenethyl cyanide [**24**, prepared from **23**])[43] to afford amines **26** and **27**, respectively. Deacetylation[40] afforded the final compounds as free-bases, which were readily converted to the water-soluble dihydrochloride salts **5** and **9**.

Aminoquinolines possessing two methylene units between the quinoline system and secondary amine (**6**, **7**, **8**, and **14**–**16**,

Scheme 2[a]

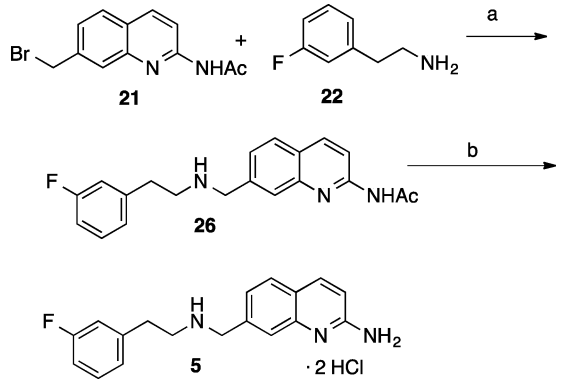

[a]Reagents and conditions: (a) Cs_2CO_3, DMF, r.t.; (b) (i) K_2CO_3, MeOH, reflux, (ii) MeOH/HCl, r.t. (after isolation).

Scheme 4) were likewise prepared from bromide **21** by homologation with cyanide ion to afford nitrile **28**. This compound was reduced to the polar quinolinyl-ethanamine (**29**) using hydrogen and Raney nickel; **29** was used crude in the next step. From this amine, benzyl analogue **6** was prepared by an "indirect" reductive amination, where **29** was treated with 3-fluorobenzaldehyde (**30**) under mildly acidic, dehydrating conditions. When the aldehyde was consumed (as measured by TLC), the dehydrating agent was filtered, and the resulting aldimine reduced by $NaBH_4$. Subsequent deacetylation, work-up, and acidification afforded **6**.

To prepare phenethyl analogues **7**, **14**, **15**, and **16** (see Scheme 4), requisite phenylacetaldehydes **35**–**38** were prepared by Dess-Martin oxidation of commercially available phenethyl alcohols **31**–**34**, respectively.[36] A "direct" reductive

dx.doi.org/10.1021/jm401838x | J. Med. Chem. 2014, 57, 1513–1530

Scheme 3[a]

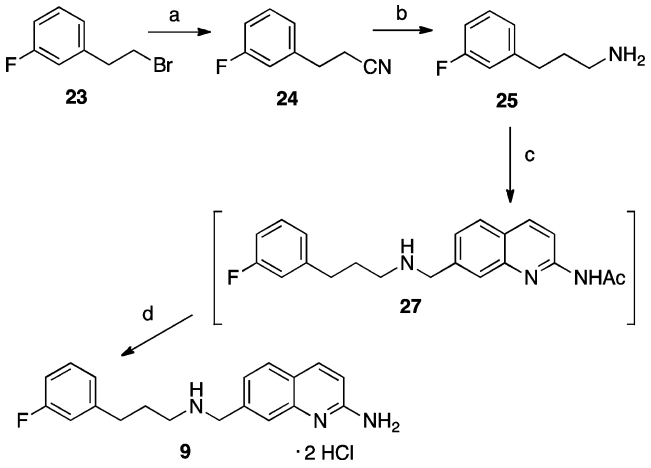

[a]Reagents and conditions: (a) NaCN, DMF, 60 °C; (b) H_2, Raney Ni NH_3/MeOH/EtOH, r.t.; (c) **21**, Cs_2CO_3, DMF, r.t.; (d) (i) K_2CO_3, MeOH, reflux, (ii) MeOH/HCl, r.t. (after isolation).

amination using **29** and the desired aldehyde was used to assemble the cores of the final analogues. Yields were low because of dialkylation and aldehyde condensation byproducts; the use of other solvents, dehydrating agents, and reductants failed to alleviate these problems; the aldehydes may be light- and acid-sensitive as well. For these analogues, the intermediate acetamides were immediately deprotected after isolation (because of some concerns about their stability) to yield **7**, **14**, **15**, and **16** and converted into dihydrochloride salts, which could be easily purified by crystallization, trituration, or preparative HPLC. Finally, the preparation of propyl analogue **8** began with 3-fluorophenylpropionic acid (**39**). Reduction to phenylpropanol **40**,[44] followed by Swern oxidation, afforded sensitive aldehyde **41**. Reductive amination using amine **29**, deacetylation, workup, and acidification afforded **8**, as also shown in Scheme 4.

6-Substituted 2-aminoquinolines were prepared similarly to those described above, beginning instead with 4′-methylcinnamanilide (**42**, Scheme 5). Using the cyclization−dearylation

Scheme 5[a]

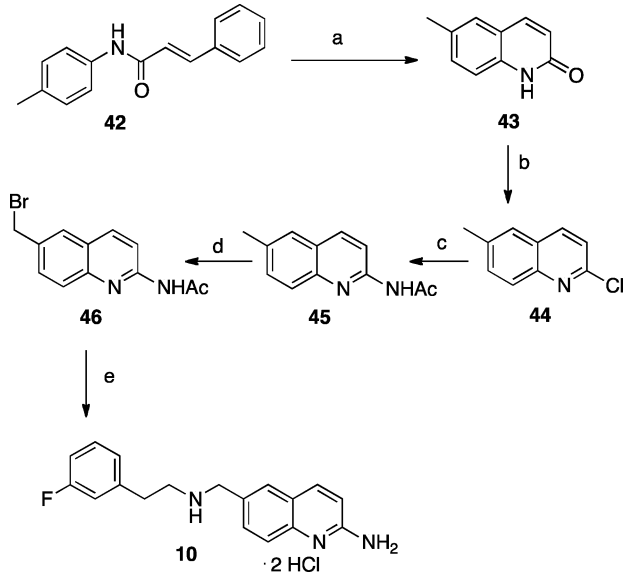

[a]Reagents and conditions: (a) $AlCl_3$, PhCl, 90 °C; (b) (i) $POCl_3$, reflux; (c) $AcNH_2$ K_2CO_3, reflux (~230 °C); (d) NBS, $(PhCO_2)_2$, benzene, reflux. (e) (i) **22**, Cs_2CO_3, DMF, r.t., (ii) K_2CO_3, MeOH, reflux (after isolation), (iii) MeOH, HCl, r.t. (after isolation).

procedure, **43** was prepared and immediately chlorinated to yield **44**.[39,40] Amidation (to yield **45**) and bromination afforded **46**. Compound **46** was treated with **22**, and the resulting acetamide was deacetylated, isolated, and acidified as before to yield **10**.

Likewise, as shown in Scheme 6, homologation of **46** with cyanide ion afforded **47**, which was readily reduced to

Scheme 4[a]

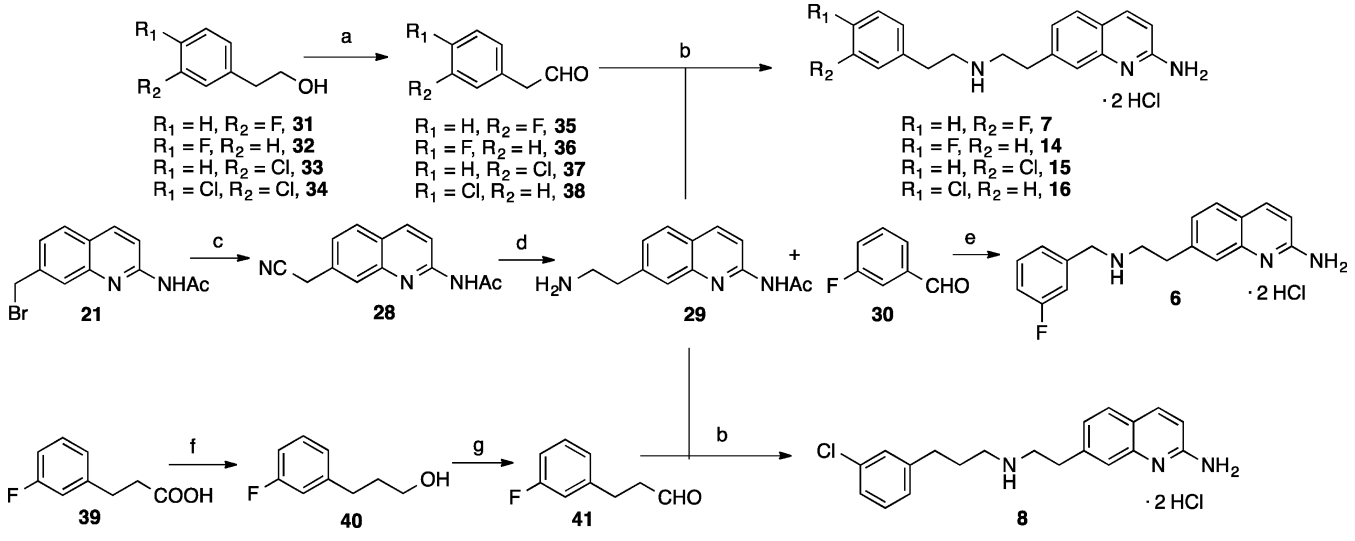

[a]Reagents and conditions: (a) Dess-Martin periodinane, CH_2Cl_2, r.t.; (b) (i) AcOH, $MgSO_4$, $CHCl_3$/MeOH, r.t.−0 °C, (ii) $Na(OAc)_3BH$, 0 °C−r.t., (iii) K_2CO_3, MeOH, reflux (after isolation), (iv) HCl, MeOH, r.t. (after isolation); (c) NaCN, DMF, r.t.; (d) H_2, Raney Ni, NH_3/MeOH/EtOH, r.t.; (e) (i) AcOH, Na_2SO_4 $CHCl_3$/MeOH, (ii) $NaBH_4$, MeOH, r.t., (iii) K_2CO_3, MeOH, reflux (after isolation), (iv) HCl, MeOH, r.t. (after isolation), (f) borane-THF, 0 °C−r.t., (g) (i) DMSO, $(COCl)_2$, −78 °C, (ii) Et_3N, −78 °C−r.t.

dx.doi.org/10.1021/jm401838x | J. Med. Chem. 2014, 57, 1513−1530

Scheme 6[a]

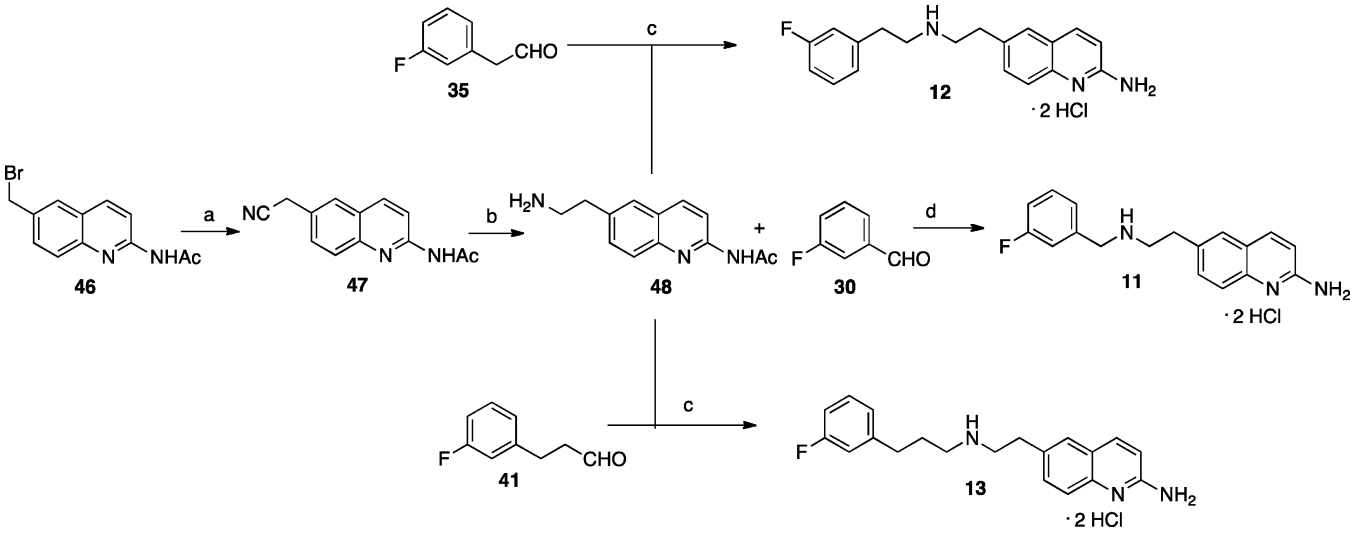

[a]Reagents and conditions: (a) NaCN, DMF r.t.; (b) H_2, Raney Ni, NH_3/MeOH/EtOH, r.t.; (c) (i) AcOH, $MgSO_4$, $CHCl_3$/MeOH, r.t.−0 °C, (ii) $Na(OAc)_3BH$, 0 °C−r.t., (iii) K_2CO_3, MeOH. reflux (after isolation), (iv) HCl, MeOH, r.t. (after isolation), (d) (i) AcOH, Na_2SO_4 $CHCl_3$/MeOH, (ii) $NaBH_4$, MeOH, r.t., (iii) K_2CO_3, MeOH, reflux (after isolation), (iv) HCl, MeOH, r.t. (after isolation).

ethanamine **48**. The indirect reductive amination procedure (using **30**) afforded **11** after deacetylation, isolation, and acidification. The direct reductive amination employing aldehyde **35** similarly afforded **12** after deacetylation/acidification, while the same reductive amination procedure using **41** instead yielded **13** after deprotection and salt formation.

RESULTS AND DISCUSSION

Compounds **5**−**16** were assayed against purified rat nNOS, bovine eNOS, and murine macrophage iNOS using the hemoglobin capture assay, as previously described.[45,46] The apparent K_i values and isoform selectivities are summarized in Table 1, and values for compounds **1**, **2**, and **3** are included for comparative purposes; the IC_{50} values and selectivities for **4** are given in Figure 1.

The lead 7-substituted 2-aminoquinoline, compound **5**, has potent nNOS inhibitory activity (74 nM) and high n/i selectivity (124-fold), yet it is only weakly selective for nNOS over eNOS (around 6-fold). The crystal structures of **5** bound to both nNOS and eNOS (Figure 3a and b, respectively) indicate that the bound conformation of **5** is virtually identical in both isoforms. In both cases, the aminoquinoline acts as an arginine mimic and interacts with the active site glutamate as arginine does (Glu592 in nNOS (1OM4); Glu363 in eNOS (2NSE)),[47] while the secondary amine sits between the heme propionates, making H-bonds to both. To simultaneously establish hydrogen bonds between the aminoquinoline and Glu592 as well as between the secondary amine and both heme propionates, the rigid quinoline plane must tilt significantly from the heme plane. The fluorophenethyl moiety, as predicted from the short linker length, does not quite reach the hydrophobic pocket (Figure 3) consisting of Tyr706, Leu337, Met336, and Trp306 in nNOS (Tyr477, Leu107, Val106, and Trp76 in eNOS). Contact with these residues is implicated in high potency and isoform selectivity.[27,35] These contacts are absent in **5**, thus resulting in poor selectivity for nNOS over eNOS; this observation is similar to that of the crystal structure of **3**.[26]

Table 1. Inhibition of NOS Enzymes by Compounds 5−16

	K_i (μM)[a]			selectivity	
compd	nNOS	iNOS	eNOS	n/i	n/e
1	0.014	4.1	28	293	2000
2	0.007	5.8	19.2	807	2676
3	0.011	1.6	0.9	149	82
5	0.075	9.14	0.485	124	6.2
6	0.254	24.5	7.77	97	30
7	0.049	44.0	11.16	899	228
8	0.164	31.9	7.25	194	44
9	0.060	32.3	3.69	538	62
10	>5.7	NT	NT	ND	ND
11	>5.7	NT	NT	ND	ND
12	>5.7	NT	NT	ND	ND
13	4.37	NT	NT	ND	ND
14	0.183	51.2	8.86	280	37
15	0.066	28.4	7.24	431	110
16	0.212	19.2	9.89	91	47

[a]The compounds were assayed for in vitro inhibition against three purified NOS isoforms: rat nNOS, bovine eNOS, and murine iNOS, using known literature methods (see Experimental Section for details), and K_i values are calculated directly from IC_{50} values. IC_{50} values are the average of at least two replicates from nine data points; all experimental standard error values are less than 14%, and all correlation coefficients are >0.81. Selectivity values are ratios of respective K_i values. NT = not tested; ND = not determined.

We sought to improve potency and isoform selectivity by elongating the chain between the aminoquinoline and the noncoordinating aryl ring (Figure 2). To this end, extra methylene groups were inserted between the secondary amine and fluorophenyl group (**9**) or between the quinoline and the secondary amine (**7**, **8**). We reasoned that moving the amine farther from the quinoline could also have the advantage of relaxing the constraints on the quinoline ring orientation but still allow the amine to interact with the heme propionates, thus, in turn, anchoring the tail in a favorable orientation to

dx.doi.org/10.1021/jm401838x | J. Med. Chem. 2014, 57, 1513−1530

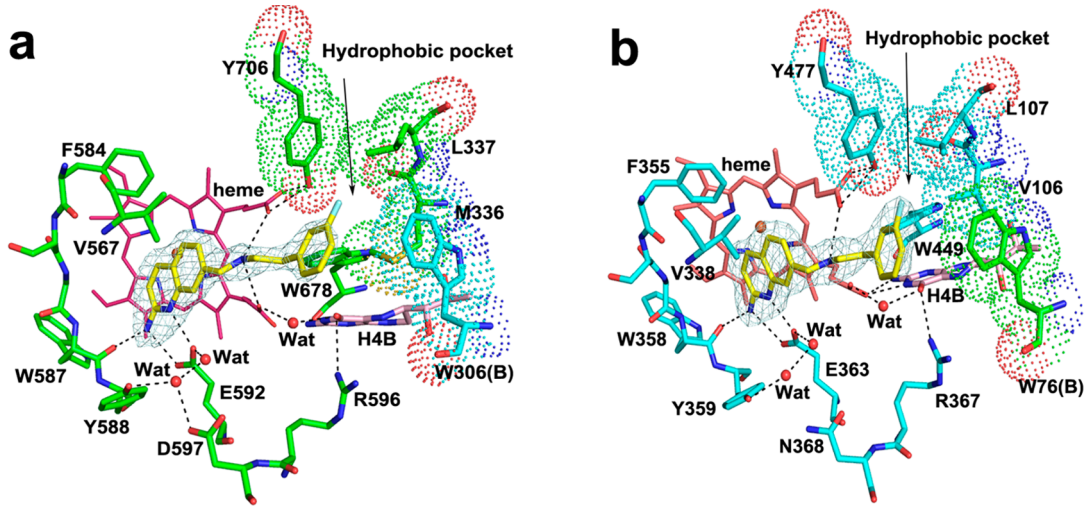

Figure 3. Active site structures of lead **5** bound to rat nNOS (a) and bovine eNOS (b). The omit $F_o - F_c$ density map for the inhibitor is shown at the 2.5 σ contour level. Major hydrogen bonds are shown as dashed lines. In each panel, the four residues that line a hydrophobic pocket are highlighted by a dot surface representation. While residues in chain A of nNOS (a) and eNOS (b) are colored green and cyan, respectively, the residue from chain B (second monomer in the homodimeric structure) is distinguished by a different color. The same color scheme is used in the other figures as well. Figures were prepared with PyMol (www.pymol.org).

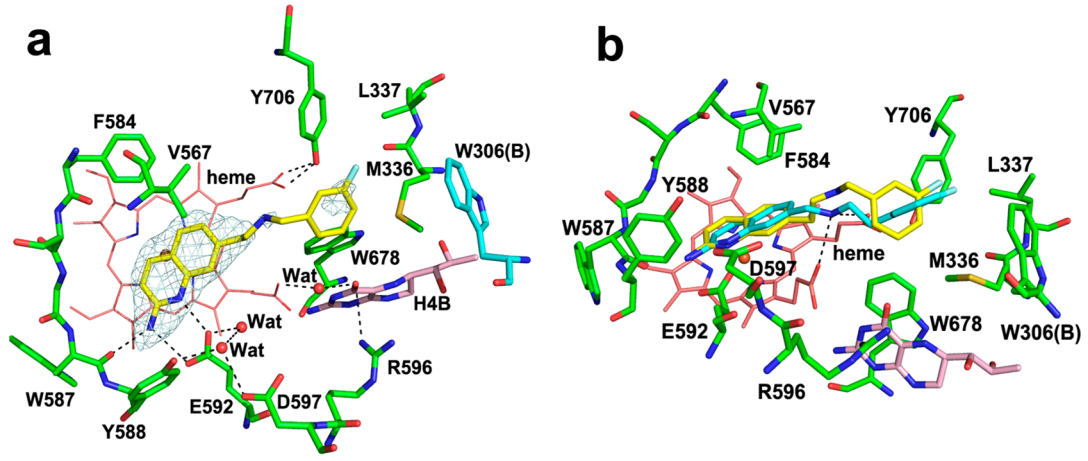

Figure 4. (a) Active site structure of **6** bound to nNOS. The omit $F_o - F_c$ density map for the inhibitor is shown at the 2.5 σ contour level. The fluorophenethyl tail is partially disordered with weaker density. (b) Overlay of **5** (cyan) and **6** (yellow) in nNOS. The different tilt angles of the aminoquinoline ring relative to the heme plane is in part related to whether hydrogen bonds (dashed lines) from the heme propionates to the linker amine are present (compound **5**) or absent (compound **6**).

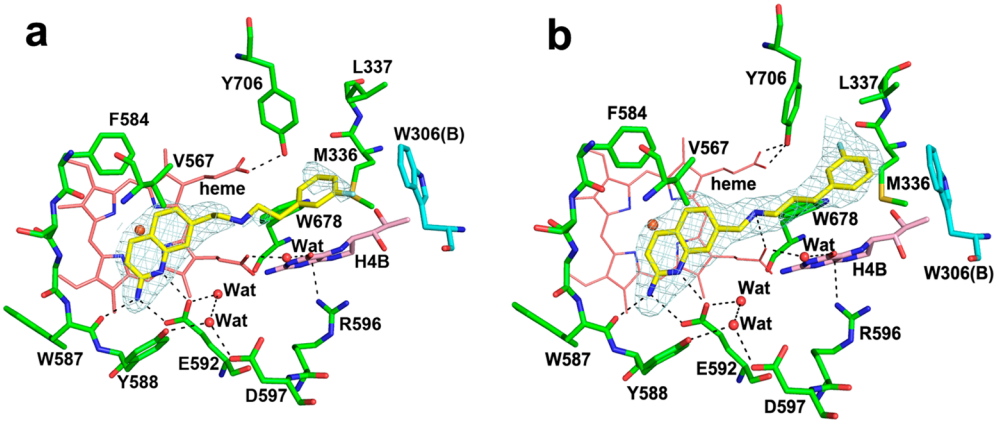

Figure 5. Active site structure of **7** (a) or **9** (b) bound to nNOS. The omit $F_o - F_c$ density map for the inhibitor is shown at the 2.5 σ contour level. The fluorophenethyl tail of **7** shows weaker density, indicative of disordering. Major hydrogen bonds are shown as dashed lines.

dx.doi.org/10.1021/jm401838x | J. Med. Chem. 2014, 57, 1513−1530

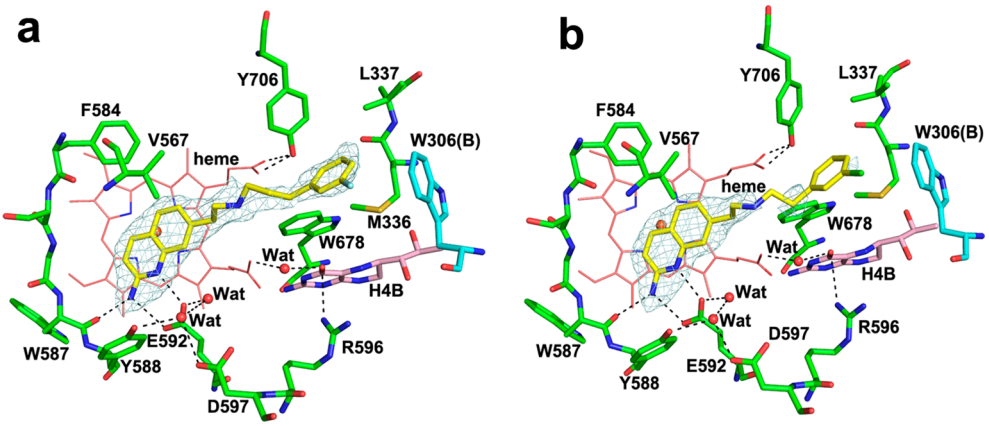

Figure 6. Active site structure of **8** (a) or **15** (b) bound to nNOS. The omit $F_o - F_c$ density map for the inhibitor is shown at the 2.5 σ contour level. The chlorophenethyl tail of **15** is partially disordered with weaker density. Major hydrogen bonds are shown as dashed lines.

make hydrophobic contacts. Following that same rationale, compound **6** was also prepared.

There are two factors that affect the comparative inhibitor potency in this series of aminoquinoline compounds: the linker length and the position of the amine group. Contrary to our prediction regarding amine position, the structure of nNOS with **6** bound (Figure 4a) reveals that placing two carbons between the quinoline and the amine actually diminishes the interaction with the heme propionates (more than 3.6 Å distance), leading to increased flexibility as evidenced by the disordered fluorophenethyl tail in the structure of **6** and decreased potency relative to **5**. Superimposition of these two nNOS structures (**5** and **6**, Figure 4b) reveals that the loose interaction between the amine of **6** and the heme propionates (lacking of H-bonds) allows the quinoline to assume a more parallel orientation (relative to the heme) than observed in the structure of **5**. However, as the 4-atom linker (of **5** and **6**) is not long enough to bring the fluorophenyl ring in contact with the aforementioned hydrophobic pocket (as in Figure 3), the majority of the stabilization results from the hydrogen bonds from the aminoquinoline and the linker amine. Therefore, **5**, with an extra hydrogen bond, is a stronger inhibitor than **6**.

In general, compounds with shorter linkers (**5** and **6**) have lower nNOS inhibitory activity than compounds with longer linkers (**7** and **9**, Table 1). The ideal chain length appears to be five atoms between the quinoline and fluorophenyl groups. nNOS inhibitory activity is very similar between **7** and **9** (Table 1) with the nitrogen placement not drastically affecting potency; it appears that the influence of the amine position is weakened in these inhibitors with longer linker lengths. The omit electron density map reveals that **7** (Figure 5a), which lacks a strong secondary amine−heme propionate interaction, is more flexible/disordered in the fluorophenyl tail region relative to the structure of **9** (which does show the amine−propionate interaction and an ordered fluorophenyl tail, like **5**). Nonetheless, the similar potencies of **7** and **9** indicate that the nitrogen position is not crucial for these compounds with longer linkers, likely because additional stabilization results from contact with the hydrophobic pocket. Indeed, the structure of **9** (Figure 5b) shows numerous favorable hydrophobic contacts between the fluorophenyl group and the nonpolar residues at the far end of the substrate access channel, Tyr706, Leu337, Met336, and Trp306 (of the other monomer of the nNOS homodimer). Although the tail of **7** (Figure 5a) is more disordered in structure than that of **9** (Figure 5b), these hydrophobic contacts exist with **7** as well. Therefore, when the linker is long enough to allow contact between the fluorophenyl ring and the hydrophobic pocket, the strong combined stabilization from both the hydrophobic interactions and the aminoquinoline−Glu592 interaction may effectively outweigh any lack of interaction between the secondary amine and heme propionates.

Chain lengths that are longer than the ideal (e.g., compound **8**, with six atoms between the quinoline and fluorophenyl group) result in a drop in potency when compared with **7** or **9**. The crystal structure with **8** (Figure 6a) shows that the fluorophenyl ring of **8** makes hydrophobic contacts similar to those of **7** and **9**. Nonetheless, to make these contacts, the flexible chain has to assume a kinked conformation, in contrast to the fully extended linker conformation seen in **9** (Figure 5b). The kinked conformation of **8** may result in unfavorable torsional strain in the linker region upon binding.

It is worth noting that 7-substituted 2-aminoquinolines are, as a whole, very poor iNOS inhibitors; an earlier report also describes the parent compound, 2-aminoquinoline, as having only weak iNOS inhibitory activity (1.7 μM).[48] Compounds **7**, **9**, and **15** have K_i values of 44 μM, 32.3 μM, and 28.4 μM, respectively, and **7** has nearly 900-fold selectivity for nNOS over iNOS, a value which is significantly higher than those of **1**−**4**, and is among the highest selectivity reported for nNOS over iNOS for nonpeptidic inhibitors. Contact with the substrate-channel hydrophobic pocket (vide supra) could be in part responsible for this high n/i selectivity. Murine iNOS contains a polar asparagine residue (Asn115)[27] in this pocket (at the position of Leu337 of nNOS) that would strongly disfavor binding by a hydrophobic group. Nonetheless, even the short-chain inhibitors (**5** and **6**) still possess good n/i selectivity, despite not reaching this distal pocket, indicating that interactions with residues at this end of the binding site are not the full determinant of this poor iNOS inhibition. It is reported that the heme-binding sites themselves differ between iNOS and nNOS isoforms,[27] with the former possessing a smaller and more rigid active site that may not tolerate the bulky and inflexible aminoquinoline as well. Interestingly, the selectivity patterns (higher n/i selectivity) contrast with many aminopyridine-based inhibitors, which have higher n/e selectivity. In some cases (such as the *R*,*R*-enantiomer of **1**), this high n/e selectivity can be explained by water-mediated contacts made between the center pyrrolidine ring and Asp597,[49] a residue that exists in both nNOS and iNOS but

dx.doi.org/10.1021/jm401838x | J. Med. Chem. 2014, 57, 1513−1530

is Asn369 in eNOS. This aspartate residue can provide considerable electrostatic or hydrogen-bonding stabilization in nNOS versus eNOS; this stabilization also manifests itself in the high n/e selectivity of dipeptide-based inhibitors,[50,51] but no contacts with Asp597 are observed in the aminoquinoline crystal structures. In other cases, high n/e selectivity is rationalized by the tighter π-stacking with Tyr706 of nNOS than with the analogous Tyr477 of eNOS, leading to greater nonbonded contacts and better desolvation.[49] While no clear π-stacking interactions are visible in the nNOS crystal structures of **6**, **7**, **8**, or **9**, hydrophobic contacts and desolvation may still play a substantial role in n/e selectivity for aminoquinolines. The binding mode of the aminoquinoline portion is identical in the structure of **7** bound to nNOS (Figure 5a) or eNOS (Figure 7) and does not contribute to isoform selectivity.

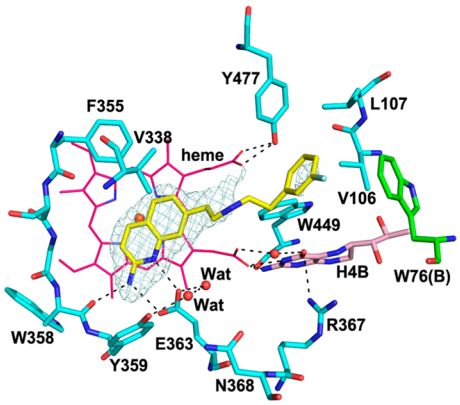

Figure 7. Active site structure of **7** bound to eNOS. The omit $F_o - F_c$ density map for the inhibitor is shown at the 2.5 σ contour level. The fluorophenethyl tail of **7** shows weaker density indicative of partial disordering. Major hydrogen bonds are shown as dashed lines.

However, the length of the linker in **7** enables the fluorophenyl ring to make good hydrophobic contacts with the residues Met336, Leu337, Tyr706, and Trp306 (from the other monomer of the nNOS homodimer). The bulky and flexible Met336 side chain makes extensive contacts with the fluorophenyl group of **7**, whereas the analogous residue, Val106 in eNOS, with a smaller surface area, cannot make that many contacts. Additionally, the side chain of Tyr706 in nNOS rotates by about 60° in order to make better contacts with the tail of **7**, while in the eNOS structure (Figure 7), Tyr477 remains in its original side chain orientation. Overall, these differences are fairly subtle but still contribute to the slightly tighter binding of **7** to nNOS over eNOS. Small changes in these hydrophobic contacts could also explain why **7** is more selective than **9**.

While 7-substituted aminoquinolines (**5**–**9** and **14**–**16**) are all highly potent against nNOS, the analogous 6-substituted aminoquinolines **10**–**13** have low potency, regardless of chain length or nitrogen position. This disparity is also explained by the crystal structures of the bound 2-aminoquinolines. In the heme-binding pocket, the aminoquinoline system does not stack parallel to the heme but rather tilts down slightly toward the "back wall" of this pocket (Figure 4a and b). In cases where an H-bond is formed between the secondary amine and heme propionates, the angle between the planes of the aminoquinoline and heme can be as large as 45°, held in this conformation by the H-bond. Even when no hydrogen bond is present, the aminoquinoline still tilts to avoid unfavorable contact with Val567 and Phe584, bulky residues that project downward from the roof of this pocket. A large or flexible substituent located at position 6, in any case, would clash directly with these bulky residues or the heme propionates, or force the rigid aminoquinoline system into a position where it can no longer be accommodated in the heme-binding pocket. This also explains why **11** has low nNOS inhibitory activity despite sharing a similar overall structure with **4** (the same number of atoms and a similar orientation between the arginine-mimic portions and the noncoordinating aryl rings). The flexibility (more rotatable bonds) of **4** allows it to be accommodated more easily in the heme-binding pocket, whereas **11** is too rigid to fit. It also was reported in the literature that rigid fused 2-aminodihydroquinoline-based nNOS inhibitors show a similar SAR regarding substituent placement; large amine-containing tails can be easily placed in the region analogous to the 7-position, whereas the area occupied by the 6-position can only fit small substituents, such as fluorine.[31−33]

Interestingly, the replacement of the fluorine in the 3-fluorophenyl group of **7** with a bulkier chlorine (compound **15**) does not significantly decrease the nNOS inhibitory potency of **15** and is only modestly detrimental to isoform selectivity, which remains 431-fold and 110-fold for iNOS and eNOS, respectively. As shown in Figure 6b, **15** binds to nNOS in a manner very similar to that of **7** (Figure 5a). Without a strong interaction between the amine and the heme propionates, the chlorophenethyl tail is partially disordered but can still be located based on the partial density contoured at 0.5 σ. In this model, the chlorine atom is not pointing directly into the hydrophobic pocket, so the switch between chlorine and fluorine should not significantly alter contacts with the enzyme. Placement of the fluorine (or chlorine) at the 4-position, however, is a disfavored modification (compare **7** to **14** or **15** to **16**). This drop in potency could arise from unfavorable steric clashes between the 4-position substituent (which would face directly toward the back of the hydrophobic pocket) and any hydrophobic pocket residue, especially Met336 and Leu337.

Encouraged by the high potency and selectivity of **7** and **15**, we assayed these compounds (and lead **5**) against purified human nNOS (Table 2). The human isoform has an active site

Table 2. Inhibition of Rat and Human nNOS by Compounds 5, 7, and 15[a]

	K_i (μM)		
compd	rat nNOS	human nNOS	selectivity (rat/human)
5	0.074	0.493	6.7
7	0.049	0.318	6.5
15	0.066	0.440	6.7

[a]See Table 1 and Experimental Section for details of the assay. K_i values are calculated directly from IC_{50} values. IC_{50} values are the average of at least two replicates from nine data points; all experimental standard error values are less than 10%, and all correlation coefficients are >0.90. Selectivity values are ratios of respective K_i values.

that is nearly identical to that in the rat enzyme,[52] with the exception of the hydrophobic pocket, where Leu337 is replaced by a histidine (His341). This pocket is smaller and more polar, and may prefer to bind inhibitors with less bulky and more hydrophilic tails. Previously, aminopyridine-based inhibitors showed lower potency against the human enzyme when compared to the rat enzyme,[35] and the same trend is observed

dx.doi.org/10.1021/jm401838x | J. Med. Chem. 2014, 57, 1513−1530

for the aminoquinolines, although **5**, **7**, and **15** still display good human nNOS inhibition. Because of the very similar selectivities (K_i-human/K_i-rat) among these three compounds, it can be concluded that the modifications that are well tolerated by the rat isoform (chain elongation and replacement of fluorine with chlorine) are likewise tolerated similarly by human nNOS, including the introduction of the bulkier chlorine.

Finally, compounds **7** and **15** were assayed in a Caco-2 monolayer permeability assay (Table 3). This assay is an approximation of both a compound's ability to penetrate the epithelium of the GI tract as well as the blood–brain barrier;[53,54] ideally, an orally bioavailable nNOS inhibitor should show high permeability in this assay. An efflux ratio (ratio of membrane permeability (A→B) to efflux (B→A)) < 3 is considered favorable. Pleasingly, both **7** and **15** display good membrane permeability in the apical to basolateral (A→B) direction and high compound recovery values. Compound **15** even shows improved membrane permeation relative to compound **4**, and both **7** and **15** display relatively low efflux ratios, diminishing the possibility that P-gp or other active transport mechanisms are significantly acting on these compounds (especially on **15**). Interestingly, compound **15** is more membrane-permeable than **7** despite their nearly identical structures; this could be the result of the higher cLogP of **15** (3.8) relative to **7** (3.2) or to variability in the assay.

Table 3. Caco-2 Permeability Summary for Select Compounds[a]

	apparent permeability (P_{app}, 10^{-6} cm s^{-1})[b]			recovery	
compd	mean A→B	mean B→A	efflux ratio	A→B	B→A
4	27.3	34.2	1.3	113%	78%
7	16.9	41.9	2.5	63%	103%
15	30.3	24.5	0.8	98%	67%
Warfarin[c]	46.8	15.7	0.3		
Ranitidine[d]	0.5	3.8	7.2		
Talinolol[e]	0.1	10.2	77.7		

[a]All assays were performed over 2 h at a concentration of 10 μM. See Experimental Section for details. [b]Apparent permeability value. [c]High permeability control. [d]Low permeability control. [e]High efflux control.

CONCLUSIONS

In summary, we have prepared a series of novel simplified 2-aminoquinolines based on the rationale that they might bind to and inhibit nNOS in a manner similar to that of amino-pyridines, while being less polar, less basic, more lipophilic, and, therefore, more bioavailable. Compounds were assayed with purified NOS enzymes, and it was revealed that 7-substituted 2-aminoquinolines are highly potent inhibitors of nNOS and that subtle modifications (such as increasing the chain length between the aminoquinoline and a noncoordinating aryl ring) can enhance potency and greatly improve isoform selectivity to >200-fold over both iNOS and eNOS. Crystal structures indicate that these compounds act as competitive arginine mimics, where the aminoquinoline moiety makes hydrogen bonds with the active-site glutamate residue, and that the noncoordinating aryl rings are stabilized in a hydrophobic pocket on the far end of the substrate access channel. Enhanced hydrophobic contacts with **7** in this pocket in nNOS, relative to that of eNOS, may also, in part, dictate the high isoform selectivity. Most promisingly, two of these highly effective compounds, **7** and **15**, show good permeability in a Caco-2 assay. These results indicate that these compounds have high potential for oral bioavailability and brain penetration and that the 7-substituted 2-aminoquinoline cores offer very promising leads for further nNOS inhibitor development.

EXPERIMENTAL SECTION

General Procedures. Anhydrous solvents (THF, CH_2Cl_2, and DMF) were distilled prior to use. The remaining solvents, reactants, and reagents were purchased from commercial vendors and were used without further purification, with the exception of acetamide, which was heated to 80 °C and dried under vacuum before use. Melting points were determined in capillary tubes using a Buchi Melting Point B-540 apparatus and are uncorrected. ^{1}H NMR spectra were recorded at 500 MHz, using a Bruker Avance III 500 (direct cryoprobe), and ^{13}C NMR spectra were obtained at 126 MHz using the same instrument. Low-resolution ESIMS was performed using a Thermo Finnigan LCQ system. High-resolution mass spectral data were obtained at the Integrated Molecular Structure Education and Research Facility (Northwestern University) on an Agilent 6210A TOF mass spectrometer in positive ion mode using electrospray ionization, with an Agilent G1312A HPLC pump and an Agilent G1367B autoinjector. Data were processed using MassHunter software, version B.02.00. Flash column chromatography was performed using an Agilent 971-FP automated flash purification system, using a Varian column station with SiliCycle cartridges (8–80 g), or manually in glass columns using SiliCycle SiliaFlash P60 40–63 μM silica gel. Analytical HPLC was performed either using a Beckman System Gold 125 solvent module and 166 Detector or an Agilent Infinity 1260 system and an injection volume of 10 μL. A Phenomenex Gemini C18 5 μm, 110 Å reverse-phase column, Gemini NX 5 μm, 100 Å column (both with dimensions of 250 mm × 4.6 mm), or Phenomenex Synergi 5 μm, polar RP column (4.6 × 50 mm) was used for all HPLC experiments. The purity of all final target compounds was found to be ≥95% by HPLC, using either isocratic elution at 70% MeOH in H_2O (with 0.1% TFA) or a gradient of 65–95% MeOH in H_2O (with 0.1% TFA) at 0.8 mL/min. When the polar RP column was used, elution was isocratic at either 50% acetonitrile in H_2O or 35% acetonitrile in H_2O at 1.5 mL/min. Preparative HPLC was performed at the Northwestern University Center for Molecular Innovation and Drug Discovery ChemCore lab, using an Agilent 1200 Series HPLC and Agilent 6120 quadrupole mass spectrometer (API-MS mode) and a Phenomenex Gemini-NX 5 μm C18 column (150 × 21.2 mm). Analytical thin-layer chromatography was performed on Silicycle extra hard 250 μM TLC plates. Compounds were visualized with short-wavelength UV light, ninhydrin, and $KMnO_4$ stain, where relevant. Compounds **17**, **35**, **36**, and **42** were prepared by literature procedures, and their spectral data are consistent with those data reported for the same.[36,38,39]

7-[(3-Fluorophenethylamino)methyl]quinolin-2-amine Dihydrochloride (5). Compound **26** (0.187 g, 0.554 mmol) was diluted in MeOH (8 mL), and K_2CO_3 (0.077 g, 0.554 mmol) was added. The mixture was heated at 50 °C for 2 h and then at reflux for an additional 1 h. The mixture was cooled and concentrated, and the residue was diluted in EtOAc (50 mL), washed with H_2O (2 × 50 mL), and dried over anhydrous sodium sulfate. The solution was concentrated, the residue was diluted in methanolic HCl (~1.4 M, 12 mL), and the mixture was heated for 3 h at 50 °C, upon which a white crystalline precipitate formed. The mixture was cooled and filtered, and additional product was obtained upon concentration of the filtrate and recrystallization of the residue from MeOH. A total of 0.140 g of product (69%) was obtained: mp 283–285 °C (dec.). ^{1}H NMR (500 MHz; DMSO-d_6): δ 14.47 (s, 1 H), 9.65 (br s, 2 H), 9.31 (br m, 1 H), 8.39 (d, J = 9.3 Hz, 1 H), 8.30 (br s, 1 H), 7.99 (d, J = 8.2 Hz, 1 H), 7.87 (s, 1 H), 7.68 (d, J = 8.5 Hz, 1 H), 7.40 (td, J = 7.8, 6.4 Hz, 1 H), 7.16–7.09 (m, 4 H), 4.36–4.35 (m, 2 H), 3.23–3.22 (m, 2 H), 3.06 (t, J = 8.1 Hz, 2 H). ^{13}C NMR (126 MHz; DMSO-d_6): δ (163.2 + 161.3, 1 C), 154.7 (1 C), 142.6 (1 C), (140.09 + 140.03, 1 C), 136.5 (1 C),

dx.doi.org/10.1021/jm401838x | J. Med. Chem. 2014, 57, 1513–1530

135.5 (1 C), (130.60 + 130.53, 1 C), 129.1 (1 C), 126.5 (1 C), (124.82 + 124.81, 1 C), 120.9 (1 C), 118.8 (1 C), (115.53 + 115.36, 1 C), 114.5 (1 C), (113.70 + 113.54, 1 C), 49.5 (1 C), 47.3 (1 C), 31.0 (1 C). ESIMS m/z (rel. intensity) 296 (MH^+, 100). HRMS calcd for $C_{18}H_{18}FN_3$, 295.1485; found, 295.1487.

7-[2-(3-Fluorobenzylamino)ethyl]quinolin-2-amine Dihydrochloride (6). To a solution of **29** (0.062 g, 0.266 mmol) in 5:1 $CHCl_3$/MeOH (6 mL) was added aldehyde **30** (0.033 g, 0.319 mmol) and anhydrous sodium sulfate (approximately 0.5 g). The mixture was stirred rapidly for 90 min, and additional Na_2SO_4 (~0.3 g) and a catalytic amount of glacial AcOH (approximately 10 μL) were added. After a total of 3 h, extra Na_2SO_4 (~0.3 g) was added. After 4 h, TLC indicated the consumption of amine **29**, the mixture was filtered to remove the Na_2SO_4, and the filter cake was washed with 10 mL of $CHCl_3$. The mixture was concentrated, the oily residue was diluted in MeOH (5 mL), then $NaBH_4$ (~0.015 g, 0.4 mmol) was added. After being stirred for 20 min at room temperature, the solution was concentrated, and the residue was partitioned between EtOAc and H_2O (20 mL each). The layers were separated, and the aqueous layer was extracted with EtOAc (20 mL). The combined organic layers were washed with sat. aq. NaCl and dried over anhydrous sodium sulfate. Concentration afforded an oily residue that was purified by flash column chromatography (SiO_2), eluting with a gradient of EtOAc to 10% MeOH in EtOAc to yield the intermediate acetamide (0.055 g, 75%, confirmed by MS), which was immediately dissolved in MeOH (6 mL). K_2CO_3 (0.023 g, 0.167 mmol) was added, and the mixture was heated to vigorous reflux for 1 h 45 min. The mixture was cooled and concentrated, and the residue was partitioned between EtOAc and 1:1 H_2O/sat. aq. NaCl (15 mL: 5 mL). The layers were separated, and the aqueous layer was extracted with EtOAc (5 mL). The combined organic layers were dried over anhydrous sodium sulfate and concentrated to yield a sticky residue that was diluted with CH_2Cl_2 (5 mL) and filtered to remove particulate matter. Methanolic HCl (~1.4 M, 2 mL) was added, the mixture was stirred for 10 min, and ether (25 mL) was added slowly until a whitish precipitate formed. This solid was collected and dried to afford the title compound as a cream-colored amorphous solid (0.052 g, 65% based on **29**): mp 278–279 °C. ^{1}H NMR (500 MHz; DMSO-d_6): δ 14.36 (s, 1 H), 9.65 (s, 2 H), 9.20 (br s, 1 H), 8.36 (d, J = 9.3 Hz, 1 H), 8.25 (br s, 1 H), 7.91 (d, J = 8.2 Hz, 1 H), 7.59 (s, 1 H), 7.51 (m, J = 5.0 Hz, 2 H), 7.44–7.39 (m, 2 H), 7.30–7.26 (m, 1 H), 7.09 (d, J = 9.3 Hz, 1 H), 4.22 (s, 2 H), 3.22 (br s, 4 H). ^{13}C NMR (126 MHz; DMSO-d_6): δ (162.9 + 160.9, 1 C), 154.3 (1 C), 142.8 (1 C), 142.4 (1 C), 135.9 (1 C), (134.63 + 134.57, 1 C), (130.76 + 130.70, 1 C), 129.1 (1 C), (126.24 + 126.22, 1 C), 125.8 (1 C), 119.8 (1 C), 117 (1 C), (116.96 + 116.79, 1 C), (115.90 + 115.73, 1 C), 113.4 (1 C), 49.2 (1 C), 47.1 (1 C), 31.6 (1 C). ESIMS m/z (rel. intensity) 296 (MH^+, 100). HRMS calcd for $C_{18}H_{18}FN_3$, 295.1485; found, 295.1487.

7-[(3-Fluorophenethylamino)ethyl]quinolin-2-amine Dihydrochloride (7). To a solution of **29** (0.74 g, 0.321 mmol) in 7:1 $CHCl_3$/MeOH (8 mL), aldehyde **35** (0.052 g, 0.375 mmol) was added, followed by glacial AcOH (7 μL) and anhydrous $MgSO_4$ (approximately 0.5 g). The mixture was stirred at room temperature for 30 min and then cooled to 0 °C. Sodium triacetoxyborohydride (0.079 g, 0.375 mmol) was added in one portion, and the mixture was slowly warmed to room temperature over 45 min, stirred 15 min at room temperature, and diluted with $CHCl_3$ (30 mL). The mixture was filtered, the filtrate was washed with sat. aq. $NaHCO_3$ (10 mL), and the aqueous layer was extracted with $CHCl_3$ (5 mL). The combined organic layers were washed with sat aq. NaCl (10 mL) and dried over anhydrous sodium sulfate. The solution was concentrated, and the residue was purified by flash column chromatography (SiO_2), eluting with a gradient of EtOAc to 18% MeOH in EtOAc to yield the intermediate acetamide as a sticky syrup (0.030 g, 25%), which was immediately dissolved in MeOH (4 mL). K_2CO_3 (0.023 g, 0.163 mmol) was added, and the mixture was heated to vigorous reflux for 2 h. The mixture was cooled and concentrated, and the residue was partitioned between EtOAc and 3:2 H_2O/sat. aq. NaCl (10 mL/5 mL). The layers were separated, and the aqueous layer was extracted with EtOAc (2 mL). The combined organic layers were washed with sat. NaCl (4 mL), dried over anhydrous sodium sulfate, concentrated to yield a sticky residue that was diluted with CH_2Cl_2 (4 mL), and filtered to remove particulate matter. Methanolic HCl (~1.4 M, 2 mL) was added, the mixture was stirred for 10 min, ether (20 mL) was added slowly, and the mixture was sonicated until a whitish precipitate formed. This solid was collected and dried to afford the title compound as a hygroscopic, cream-colored amorphous solid (0.023 g, 18% based on **29**): mp 247–249 °C (dec). ^{1}H NMR (500 MHz; DMSO-d_6): δ 14.34 (s, 1 H), 9.21 (br s, 3 H), 8.37 (d, J = 9.3 Hz, 1 H), 8.27 (br s, 1 H), 7.92 (d, J = 8.2 Hz, 1 H), 7.60 (s, 1 H), 7.43–7.38 (m, 2 H), 7.18–7.08 (m, 4 H), 3.25–3.16 (m, 6 H), 3.02 (t, J = 8.1 Hz, 2 H). ^{13}C NMR (126 MHz; DMSO-d_6): δ (163.7 + 161.8, 1 C), 154.8 (1 C), 143.3 (1 C), 142.9 (1 C), (140.55 + 140.49, 1 C), 136.4 (1 C), (131.07 + 131.00, 1 C), 129.6 (1 C), 126.3 (1 C), (125.35 + 125.33, 1 C), 120.2 (1 C), 117.5 (1 C), (116.03 + 115.86 1 C), (114.19 + 114.02, 1 C), 113.86 (1 C), 47.7 (1 C), 32.1 (1 C), 31.6 (1 C). ESIMS m/z (rel. intensity) 310 (MH^+, 65). HRMS calcd for $C_{19}H_{20}FN_3$, 309.1641; found, 309.1645.

7-{2-[3-(3-Fluorophenyl(propylamino)ethyl]}quinolin-2-amine Dihydrochloride (8). Compound **29** (0.064 g, 0.280 mmol) was diluted in 7:1 $CHCl_3$/MeOH (7 mL), and aldehyde **41** (0.049 g, 0.322 mmol) was added, followed by glacial acetic acid (6 μL) and anhydrous $MgSO_4$ (~0.5 g). The mixture was stirred for 30 min, cooled to 0 °C, and sodium triacetoxyborohydride (~0.070 g, 0.333 mmol) was added in one portion. The mixture was allowed to warm to room temperature slowly over 50 min and was diluted with $CHCl_3$ (to a volume of approximately 50 mL) and filtered. The yellow filtrate was washed with sat. aq. $NaHCO_3$ (8 mL), and the aqueous layer was extracted with $CHCl_3$ (5 mL). The organic phase was washed with sat. aq. NaCl (10 mL), dried over anhydrous sodium sulfate, and concentrated. The resulting residue was purified by flash column chromatography (SiO_2) eluting with a gradient of EtOAc to 17% MeOH in EtOAc to yield the intermediate acetamide (0.045 g, 44%) as a sticky semisolid. This substance was immediately diluted with anhydrous MeOH (6 mL), and K_2CO_3 (0.034 g, 0.246 mmol) was added. The mixture was heated at reflux for 1 h 50 min, cooled, and concentrated. The residue was diluted with EtOAc (10 mL), and the solution was washed with H_2O/sat. aq. NaCl (1:1, 6 mL). The organic layers were washed with sat. aq. NaCl (5 mL), dried over anhydrous sodium sulfate, and concentrated. The resulting syrup was diluted in CH_2Cl_2 (3 mL) and filtered to remove particulate matter, and methanolic HCl was added (~1.4 M, 3 mL) and the mixture stirred at room temperature for 10 min. Ether (30 mL) was added, the mixture was sonicated, concentrated, and the residue was washed twice with ether (2 mL each) to afford the product as a cream-colored hygroscopic solid (0.042 g, 37% from **29**): mp 81–83 °C (softens), 210 °C (dec). ^{1}H NMR (500 MHz; DMSO-d_6): δ 14.31 (s, 1 H), 9.21–9.13 (m, 3 H), 8.37 (d, J = 9.3 Hz, 1 H), 8.25 (br s, 1 H), 7.91 (d, J = 8.2 Hz, 1 H), 7.59 (s, 1 H), 7.42 (dd, J = 8.2, 1.3 Hz, 1 H), 7.38–7.34 (m, 1 H), 7.12–7.03 (m, 4 H), 3.21–3.14 (m, 4 H), 2.95–2.90 (m, 2 H), 2.71 (t, J = 7.6 Hz, 2 H), 1.96 (dt, J = 15.3, 7.7 Hz, 2 H). ^{13}C NMR (126 MHz; DMSO-d_6): δ (163.2 + 161.3, 1 C), 154.3 (1 C), (143.71 + 143.65, 1 C), 142.8 (1 C), 142.5 (1 C), 135.8 (1 C), (130.32 + 130.25, 1 C), 129.1 (1 C), 125.8 (1 C), (124.47 + 124.45, 1 C), 119.7 (1 C), 117.0 (1 C), (115.09 + 114.92, 1 C), 113.4 (1 C), (112.95 + 112.79, 1 C), 47.1 (1 C), 46.1 (1 C), 31.73 (1 C), 31.54 (1 C), 26.8 (1 C). ESIMS m/z (rel. intensity) 324 (MH^+, 28). HRMS calcd for $C_{20}H_{22}FN_3$, 323.1798; found, 323.1800.

7-{2-[3-(3-Fluorophenyl(propylamino)methyl]}quinolin-2-amine Dihydrochloride (9). Anhydrous Cs_2CO_3 (0.105 g, 0.322 mmol) was diluted with anhydrous DMF (3 mL), **25** (0.050 g, 0.322 mmol) was added as a solution in DMF (~2 mL), and the mixture was stirred for 30 min at room temperature. Compound **21** (0.075 g, 0.269 mmol) was then added as a solution in DMF (1.3 mL) over several minutes. The mixture was stirred at room temperature for 16 h and then concentrated. The residue was partitioned between EtOAc and H_2O (10 mL each), the layers were separated, and the aqueous layer was saturated with NaCl and extracted with EtOAc (2 × 5 mL). The combined organic layers were washed with sat. aq. NaCl (10 mL), dried over anhydrous sodium sulfate, and concentrated. The residue

was purified by flash column chromatography (SiO_2), eluting with a gradient of EtOAc to 15% MeOH in EtOAc to yield **27** as a yellow syrup (0.039 g, 41%), which was used without further characterization. This compound was diluted with anhydrous MeOH (6 mL), and anhydrous K_2CO_3 (0.031 g, 0.022 mmol) was added. The mixture was heated at reflux for 2 h 15 min, cooled, and concentrated. The residue was diluted with EtOAc (10 mL), and 3 mL each of H_2O and sat. aq. NaCl was added. The layers were separated, the aqueous layer was extracted with EtOAc (3 × 4 mL), and the combined organic layers were washed with sat. aq. NaCl (4 mL), dried over anhydrous sodium sulfate, and concentrated. The residue was diluted with CH_2Cl_2 (5 mL), filtered to remove particulate matter, and reconcentrated. Methanolic HCl (~1.4 M, 3 mL) was added, the mixture was stirred for 5 min, and ether (30 mL) was added slowly until a white precipitate formed. This solid was collected and dried to afford the title compound as a white microcrystalline solid (0.029 g, 28% based on **21**) after drying in vacuo: mp 250−252 °C (dec). ^{1}H NMR (500 MHz; DMSO-d_6): δ 14.44 (s, 1 H), 9.50 (s, 2 H), 9.30 (br s, 1 H), 8.39 (d, J = 9.2 Hz, 1 H), 8.30 (br s, 1 H), 7.98 (d, J = 8.2 Hz, 1 H), 7.86 (s, 1 H), 7.66 (d, J = 8.3 Hz, 1 H), 7.35 (td, J = 8.0, 6.4 Hz, 1 H), 7.15 (d, J = 9.3 Hz, 1 H), 7.10−7.02 (m, 3 H), 4.32 (t, J = 5.5 Hz, 2 H), 2.95−2.90 (m, 2 H), 2.70 (t, J = 7.6 Hz, 2 H), 2.00 (quintet, J = 7.7 Hz, 2 H). ^{13}C NMR (126 MHz; DMSO-d_6): δ (163.2 + 161.3, 1 C), 154.6 (1 C), (143.67 + 143.61, 1 C), 142.6 (1 C), 136.6 (1 C), (130.32 + 130.25, 1 C), 129.0 (1 C), 126.4 (1 C), (124.47 + 124.45, 1 C), 120.9 (1 C), 118.7 (1 C), (115.08 + 114.91, 1 C), 114.5 (1 C), (112.95 + 112.78, 1 C), 49.3 (1 C), 46.0 (1 C), 31.5 (1 C), 26.7 (1 C); one of the aminoquinoline carbons is not visible due to baseline broadening; ESIMS m/z (rel. intensity) 310 (MH^+, 100). HRMS calcd for $C_{19}H_{20}FN_3$, 309.1641; found, 309.1645.

6-[(3-Fluorophenethylamino)methyl]quinolin-2-amine Dihydrochloride (10). Anhydrous Cs_2CO_3 (0.090 g, 0.288 mmol) was diluted in anhydrous DMF (5 mL), and amine **22** (0.040 g, 0.288 mmol) was added. The mixture was stirred for 30 min at room temperature before compound **46** (0.070 g, 0.250 mmol) was added dropwise as a solution in anhydrous DMF (2 mL). The resultant suspension was stirred for 16 h at room temperature and concentrated, the residue was partitioned between EtOAc and H_2O (5 mL each), and the layers were separated. The aqueous layer was extracted with EtOAc (2 × 5 mL), and the organic layers were washed with sat. aq. NaCl (5 mL), dried over anhydrous sodium sulfate, and concentrated. The residue was purified by flash column chromatography (SiO_2), eluting with a gradient of EtOAc to 10% MeOH in EtOAc to yield the intermediate acetamide as a yellow syrup (0.040 g, 47%, confirmed by MS). This syrup was dissolved in MeOH (5 mL), and K_2CO_3 (0.026 g, 0.148 mmol) was added. The mixture was heated at reflux for 2 h, cooled to room temperature, and concentrated. The residue was partitioned between EtOAc (5 mL) and sat. aq. NaCl/H_2O (4:1, 5 mL). The layers were separated, and the aqueous layer was extracted with EtOAc (2 × 5 mL). The combined organic phase was washed with sat aq. NaCl (4 mL), dried over anhydrous sodium sulfate, and concentrated. The resulting residue was diluted in CH_2Cl_2 (5 mL) and filtered to remove particulate matter, and methanolic HCl (~1.4 M, 3 mL) was added. After 10 min, ether (20 mL) was added, and a precipitate formed. This was collected and dried to yield the title compound as a cream-colored powder (0.036 g, 38% from **46**: mp 277−278 °C). ^{1}H NMR (500 MHz; DMSO-d_6): δ 14.35 (s, 1 H), 9.58 (s, 2 H), 9.28 (br s, 1 H), 8.37 (d, J = 9.5 Hz, 1 H), 8.32 (br s, 1 H), 8.05 (s, 1 H), 7.96 (d, J = 8.6 Hz, 1 H), 7.78 (d, J = 8.5 Hz, 1 H), 7.39 (td, J = 7.8, 6.4 Hz, 1 H), 7.16−7.09 (m, 4 H), 4.29 (s, 2 H), 3.20−3.19 (m, 2 H), 3.05 (t, J = 8.1 Hz, 2 H). ^{13}C NMR (126 MHz; DMSO-d_6): δ (163.2 + 161.2, 1 C), 154.4 (1 C), 142.8 (1 C), (140.11 + 140.05, 1 C), 135.9 (1 C), 134.2 (1 C), 130.59 (1 C), (130.58 + 130.52, 1 C), 128.6 (1 C), (124.83 + 124.81, 1 C), 120.5 (1 C), 117.6 (1 C), (115.53 + 115.36, 1 C) 114.5 (1 C), (113.69 + 113.52, 1 C), 49.2 (1 C), 47.0 (1 C), 31.0 (1 C). ESIMS m/z (rel. intensity) 296 (MH^+, 100). HRMS calcd for $C_{18}H_{18}FN_3$, 295.1485; found, 295.1490.

6-[2-(3-Fluorobenzylamino)ethyl]quinolin-2-amine Dihydrochloride (11). Amine **48** (0.050 g, 0.218 mmol) was dissolved in anhydrous $CHCl_3$ (3 mL), and aldehyde **30** (0.034 g, 0.274 mmol) was added, followed by 3 mL of a 2:1 mixture of $CHCl_3$/MeOH and anhydrous sodium sulfate (~0.5 g). The mixture was stirred rapidly at room temperature for 90 min, after which glacial acetic acid (10 μL) was added. After a total of 4 h, the amine appeared to be consumed by TLC, and the mixture was filtered to remove the sodium sulfate. The filtrate was concentrated, and the oily residue was diluted in MeOH (5 mL). $NaBH_4$ (0.020 g, 0.523 mmol) was added, and the mixture was stirred for 40 min at room temperature. The mixture was concentrated and partitioned between EtOAc and H_2O (10 mL of each). The layers were separated, and the aqueous layer was extracted with EtOAc (10 mL). The organic layer was washed with H_2O and sat aq. NaCl (20 mL each), dried over anhydrous sodium sulfate, and concentrated. The residue was purified by flash column chromatography (SiO_2), eluting with a gradient of EtOAc to 20% MeOH in EtOAc to yield the intermediate acetamide as a yellow syrup (0.052 g, 72%, confirmed by MS). This compound was immediately diluted in MeOH (5 mL), and K_2CO_3 (0.021 g, 0.154 mmol) was added. The mixture was heated at vigorous reflux for 2 h, cooled, and concentrated, and the resulting residue was diluted with EtOAc (20 mL) and washed with H_2O (10 mL). The aqueous layer was extracted with EtOAc (2 × 10 mL), and the combined organic layers were washed with sat. aq. NaCl (10 mL) and dried over anhydrous sodium sulfate. Concentration afforded a white solid, which was diluted with methanolic HCl (~1.4 M, 3 mL) and stirred for 10 min. The addition of ether (50 mL) resulted in the precipitation of a solid that was collected, washed with ether (20 mL) and dried in vacuo to yield the title compound as a white solid (0.043 g, 54% from **48**): mp 282−284 °C. ^{1}H NMR (500 MHz; DMSO-d_6): δ 14.24 (s, 1 H), 9.62 (s, 2 H), 9.16 (br s, 1 H), 8.35 (d, J = 9.4 Hz, 1 H), 8.19 (br s, 1 H), 7.80 (d, J = 0.7 Hz, 1 H), 7.71−7.67 (m, 2 H), 7.52−7.48 (m, 2 H), 7.42 (d, J = 7.7 Hz, 1 H), 7.30−7.26 (m, 1 H), 7.12 (d, J = 9.3 Hz, 1 H), 4.22 (s, 2 H), 3.17−3.14 (m, 4 H). ^{13}C NMR (126 MHz; DMSO-d_6): δ (162.9 + 160.9, 1 C), 154.0 (1 C), 142.8 (1 C), (134.62 + 134.56, 1 C), 134.0 (1 C), 133.3 (1 C), (130.76 + 130.70, 1 C), 128.3 (1 C), (126.24 + 126.22, 1 C), 121.0 (1 C), 117.7 (1 C), (116.96 + 116.79, 1 C), (115.90 + 115.74, 1 C), 114.0 (1 C), 49.2 (1 C), 47.2 (1 C), 30.8 (1 C); one of the aminoquinoline carbons is not visible because of baseline broadening; ESIMS m/z (rel. intensity) 296 (MH^+,100). HRMS calcd for $C_{18}H_{18}FN_3$, 295.1485; found, 295.1486.

6-[(3-Fluorophenethylamino)ethyl]quinolin-2-amine Dihydrochloride (12). To a solution of **48** (0.074 g, 0.321 mmol) in 7:1 $CHCl_3$/MeOH (8 mL), aldehyde **35** (0.049 g, 0.353 mmol) was added, followed by glacial AcOH (7 μL) and anhydrous $MgSO_4$ (approx 0.5 g). The mixture was stirred at room temperature for 20 min and then cooled to 0 °C. Sodium triacetoxyborohydride (0.082 g, 0.385 mmol) was added in one portion, and the mixture was slowly warmed to room temperature over 50 min, then diluted with CH_2Cl_2 (10 mL). The mixture was filtered, the filtrate was washed with sat. aq. $NaHCO_3$ (2 × 20 mL), and the aqueous layer was extracted with CH_2Cl_2 (2 × 10 mL). The combined organic layers were washed with sat. aq. NaCl (10 mL) and dried over anhydrous sodium sulfate. The solution was concentrated, and the residue was purified by flash column chromatography (SiO_2), eluting with a gradient of EtOAc to 20% MeOH in EtOAc to yield the intermediate acetamide as a sticky syrup (0.039 g, 34%) that was immediately dissolved in MeOH (3 mL). K_2CO_3 (0.023 g, 0.167 mmol) was added, and the mixture was heated to vigorous reflux for 1 h 50 min. The mixture was cooled and concentrated, and the residue was partitioned between EtOAc (10 mL) and 1:1 H_2O/sat. aq. NaCl (4 mL). The layers were separated, and the aqueous layer was extracted with EtOAc (2 × 4 mL). The combined organic layers were washed with sat. aq. NaCl (4 mL), dried over anhydrous sodium sulfate, and concentrated to yield a sticky residue that was diluted with CH_2Cl_2 (3 mL) and filtered to remove particulate matter. Methanolic HCl (~1.4 M, 2 mL) was added, the mixture was stirred for 10 min and concentrated, and the residue was recrystallized from 1:1 MeOH/ether (1 mL) to yield the product as a pale tan hygroscopic solid (0.025 g, 21% based on **48**): mp 223−226 °C (dec). ^{1}H NMR (500 MHz; DMSO-d_6): δ 14.37 (s, 1 H), 9.35−9.23 (m, 3 H), 8.36 (d, J = 9.4 Hz, 1 H), 8.30 (br s, 1 H), 7.83 (s, 1 H), 7.73−7.69 (m, 2 H), 7.42−7.38 (m, 1 H), 7.18−7.09 (m, 4 H),

3.22−3.19 (m, 4 H), 3.14 (t, J = 7.9 Hz, 2 H), 3.04 (t, J = 8.1 Hz, 2 H). ^{13}C NMR (126 MHz; DMSO-d_6): δ (163.2 + 161.3, 1 C), 154.0 (1 C), 142.8 (1 C), (140.14 + 140.08, 1 C), 134.6 (1 C), 134.1 (1 C), 133.3 (1 C), (130.58 + 130.51, 1 C), 128.3 (1 C), (124.86 + 124.84, 1 C), 120.9 (1 C), 117.5 (1 C), (115.54 + 115.37, 1 C), 114.0 (1 C), (113.68 + 113.52, 1 C), 47.35 (1 C), 47.20 (1 C), 31.0 (1 C), 30.8 (1 C). ESIMS m/z (rel. intensity) 310 (MH^+, 100). HRMS calcd for $C_{19}H_{20}FN_3$, 309.1641; found, 309.1647.

6-{2-[3-(3-Fluorophenyl(propylamino)ethyl]}quinolin-2-amine Dihydrochloride (13). To a solution of **48** (0.060 g, 0.261 mmol) in 10:1 $CHCl_3$/MeOH (5 mL), aldehyde **41** (0.047 g, 0.313 mmol) was added, followed by glacial AcOH (6 μL) and anhydrous $MgSO_4$ (approx 0.5 g). The mixture was stirred at room temperature for 25 min and then cooled to 0 °C. Sodium triacetoxyborohydride (0.070 g, 0.332 mmol) was added in one portion, and the mixture was slowly warmed to room temperature over 30 min, filtered, and concentrated. The residue was purified by flash column chromatography (SiO_2), eluting with a gradient of EtOAc to 20% MeOH in EtOAc to yield a sticky yellow solid (0.036 g, 27%). This substance was immediately dissolved in MeOH (3 mL), K_2CO_3 (0.030 g, 0.217 mmol) was added, and the mixture was heated to vigorous reflux for 2 h. The mixture was cooled and concentrated, and the residue was partitioned between EtOAc (6 mL) and 1:1 H_2O/sat. aq. NaCl (2 mL). The layers were separated, and the aqueous layer was extracted with EtOAc (2 × 3 mL). The combined organic layers were washed with sat. aq. NaCl (3 mL), dried over anhydrous sodium sulfate, and concentrated to yield a sticky residue that was diluted with CH_2Cl_2 (3 mL) and filtered to remove particulate matter. Methanolic HCl (∼1.4 M, 2 mL) was added, the mixture was stirred for 10 min, concentrated, and the residue was washed with 1:1 CH_2Cl_2/ether (3 mL) to yield the product as a yellow-green hygroscopic solid (0.033 g, 32% based on **48**): mp 70 °C (softens), 211−213 °C (dec). ^{1}H NMR (500 MHz; DMSO-d_6): δ 14.31 (s, 1 H), 9.20 (br s, 3 H), 8.34 (d, J = 9.4 Hz, 1 H), 8.22 (br s, 1 H), 7.82 (s, 1 H), 7.70 (s, 2 H), 7.38−7.33 (m, 1 H), 7.14−7.03 (m, 4 H), 3.23−3.17 (m, 2 H), 3.11 (t, J = 7.8 Hz, 2 H), 2.94−2.89 (m, 2 H), 2.71 (t, J = 7.6 Hz, 2 H), 1.97 (quintet, J = 7.6 Hz, 2 H). ^{13}C NMR (126 MHz; DMSO-d_6): δ (163.2 + 161.3, 1 C), 154.0 (1 C), (143.72 + 143.66, 1 C), 142.8 (1 C), 134.6 (1 C), 134.1 (1 C), 133.3 (1 C), (130.31 + 130.25, 1 C), 128.2 (1 C), (124.47 + 124.45, 1 C), 120.9 (1 C), 117.5 (1 C), (115.09 + 114.93, 1 C), 114.0, (112.95 + 112.78, 1 C), 47.3 (1 C), 46.1 (1 C), 31.5 (1 C), 30.9 (1 C), 26.8 (1 C). ESIMS m/z (rel. intensity) 325 (MH^+, 100). HRMS calcd for $C_{20}H_{22}FN_3$, 323.1798; found, 323.1803.

7-[(4-Fluorophenethylamino)ethyl]quinolin-2-amine Dihydrochloride (14). Compound **29** (0.076 g, 0.333 mmol) was diluted in 7:1 $CHCl_3$/MeOH (7 mL), and aldehyde **36** (0.045 g, 0.327 mmol) was added as a solution in 1 mL of $CHCl_3$, followed by glacial acetic acid (7 μL) and anhydrous $MgSO_4$ (∼0.5 g). The flask was sheathed with aluminum foil, and the mixture was stirred for 45 min and cooled to 0 °C, and sodium triacetoxyborohydride (0.085 g, 0.401 mmol) was added in one portion. The mixture was allowed to warm to room temperature slowly over 1 h and 15 min and was diluted with $CHCl_3$ (to a volume of approximately 50 mL) and filtered. The yellow filtrate was washed with sat. aq. $NaHCO_3$ (10 mL), and the aqueous layer was extracted with $CHCl_3$ (2 × 5 mL). The organic phase was washed with sat. aq. NaCl (20 mL), dried over anhydrous sodium sulfate, and concentrated. The resulting residue was purified by flash column chromatography (SiO_2) eluting with a gradient of EtOAc to 14% MeOH in EtOAc to yield the intermediate acetamide (0.051 g, 44%) as an oil that began to solidify on standing. This substance was immediately diluted with anhydrous MeOH (8 mL), and K_2CO_3 (0.030 g, 0.217 mmol) was added. The mixture was heated at reflux for 2 h, cooled, and concentrated. The residue was diluted with EtOAc (10 mL), and the solution was washed with H_2O/sat. aq. NaCl (1:1, 6 mL). The aqueous layer was extracted with EtOAc (3 × 6 mL), and the combined organic layers were washed with sat. aq. NaCl (6 mL), dried over anhydrous sodium sulfate, and concentrated. The resulting syrup was diluted in CH_2Cl_2 (5 mL), filtered to remove particulate matter, and reconcentrated. To the residue was added methanolic HCl (∼1.4 M, 1 mL), and the mixture was stirred at room temperature for 1 h, upon which a white crystalline solid formed. The mixture was cooled to −30 °C and filtered to yield the title compound as white flocculent crystals (0.021 g, 16% from **29**): mp 279−281 °C. ^{1}H NMR (500 MHz; DMSO-d_6): δ 14.34 (s, 1 H), 9.20 (s, 3 H), 8.37 (d, J = 9.3 Hz, 1 H), 8.26−8.24 (br s, 1 H), 7.92 (d, J = 8.2 Hz, 1 H), 7.60 (s, 1 H), 7.42 (dd, J = 8.2, 1.2 Hz, 1 H), 7.33 (td, J = 6.1, 2.5 Hz, 2 H), 7.21−7.17 (m, 2 H), 7.09 (d, J = 9.3 Hz, 1 H), 3.26−3.16 (m, 6 H), 2.98 (t, J = 8.1 Hz, 2 H). ^{13}C NMR (126 MHz; DMSO-d_6): δ (162.1 + 160.2 1 C), 154.3 (1 C), 142.8 (1 C), 142.4 (1C), 135.9 (1 C), (133.34 + 133.32, 1 C), (130.59 + 130.53, 1 C), 129.1 (1 C), 125.8 (1 C), 119.7 (1 C), 117.0 (1 C), (115.45 + 115.28, 1 C), 113.4 (1 C), 47.7 (1 C), 47.2 (1 C), 31.7 (1 C), 30.7 (1 C). ESIMS m/z (rel. intensity) 310 (MH^+, 100). HRMS calcd for $C_{19}H_{20}FN_3$, 309.1641; found, 309.1644.

7-[(3-Chlorophenethylamino)ethyl]quinolin-2-amine Dihydrochloride (15). Compound **29** (0.076 g, 0.333 mmol) was diluted in 8:1 $CHCl_3$/MeOH (7 mL), and aldehyde **37** (0.051 g, 0.330 mmol) was added as a solution in 1 mL of $CHCl_3$, followed by glacial acetic acid (7 μL) and anhydrous $MgSO_4$ (∼0.5 g). The mixture was stirred for 30 min, and cooled to 0 °C, and sodium triacetoxyborohydride (0.085 g, 0.401 mmol) was added in one portion. The mixture was allowed to warm to room temperature slowly over 1 h and was diluted with $CHCl_3$ (to a volume of approximately 50 mL) and filtered. The yellow filtrate was washed with sat. aq. $NaHCO_3$ (10 mL), and the aqueous layer was extracted with $CHCl_3$ (10 mL). The organic phase was washed with sat. aq. NaCl (20 mL), dried over anhydrous sodium sulfate, and concentrated. The resulting residue was purified by flash column chromatography (SiO_2) eluting with a gradient of EtOAc to 13% MeOH in EtOAc to yield the intermediate acetamide (0.039 g, 32%) as a semisolid. This substance was diluted with anhydrous MeOH (6 mL), and K_2CO_3 (0.029 g, 0.210 mmol) was added. The mixture was heated at reflux for 2 h, cooled, and concentrated. The residue was immediately diluted with EtOAc (10 mL), and the solution was washed with H_2O/sat. aq. NaCl (3:5, 8 mL). The organic layers were washed with sat. aq. NaCl (5 mL), dried over anhydrous sodium sulfate, and concentrated. The resulting syrup was diluted in CH_2Cl_2 (5 mL), filtered to remove particulate matter, and reconcentrated. To the residue was added methanolic HCl (∼1.4 M, 3 mL), the mixture was stirred at room temperature for 5 min, and ether (20 mL) was added, upon which an off-white solid (0.030 g, 23%) was collected. An analytically pure sample for assay was prepared by preparative LC-MS, using the instrument and column detailed in the General Procedures section, eluting with a gradient of 95% H_2O + 0.1%/formic acid 5% MeCN + 0.1% formic acid for 2 min, to 70% H_2O at 27 min, then to 0% H_2O at 32 min. Evaporation and retreatment of the residue with methanolic HCl (1 mL) and ether (1 mL) afforded the pure compound as a white flocculent solid (0.014 g, 11% from **29**): mp 281−282 °C. ^{1}H NMR (500 MHz; DMSO-d_6): δ 14.29 (s, 1 H), 9.17 (br s, 3 H), 8.37 (d, J = 9.3 Hz, 1 H), 8.25 (br s, 1 H), 7.92 (d, J = 8.2 Hz, 1 H), 7.60 (s, 1 H), 7.44−7.34 (m, 4 H), 7.27 (d, J = 7.4 Hz, 1 H), 7.09 (d, J = 9.3 Hz, 1 H), 3.25−3.20 (m, 4 H), 3.20−3.16 (m, 2 H), 3.00 (t, J = 8.1 Hz, 2 H). ^{13}C NMR (126 MHz; DMSO-d_6): δ 154.3 (1 C), 142.8 (1 C), 142.5 (1 C), 139.8 (1 C), 135.8 (1 C), 133.2 (1 C), 130.5 (1 C), 129.1 (1 C), 128.6 (1 C), 127.5 (1 C), 126.8 (1 C), 125.8 (1 C), 119.7 (1 C), 116.9 (1 C), 113.4 (1 C), 47.2 (1 C), 31.6 (1 C), 31.0 (1 C). ESIMS m/z (rel. intensity) 326 (MH^+, 100). HRMS calcd for $C_{19}H_{20}ClN_3$, 325.1346; found, 325.1352.

7-[(4-Chlorophenethylamino)ethyl]quinolin-2-amine Dihydrochloride (16). Compound **29** (0.076 g, 0.333 mmol) was diluted in 7:1 $CHCl_3$/MeOH (7 mL), and aldehyde **38** (0.051 g, 0.330 mmol) was added as a solution in 1 mL of $CHCl_3$, followed by glacial acetic acid (7 μL) and anhydrous $MgSO_4$ (∼0.5 g). The mixture was stirred for 30 min and cooled to 0 °C, and sodium triacetoxyborohydride (0.085 g, 0.401 mmol) was added in one portion. The mixture was allowed to warm to room temperature slowly over 1 h 15 min and was diluted with $CHCl_3$ (to a volume of approximately 50 mL) and filtered. The yellow filtrate was washed with sat. aq. $NaHCO_3$ (10 mL), and the aqueous layer was extracted with $CHCl_3$ (2 × 5 mL). The organic phase was washed with sat. aq. NaCl (20 mL), dried over

anhydrous sodium sulfate, and concentrated. The resulting residue was purified by flash column chromatography (SiO_2) eluting with a gradient of EtOAc to 13% MeOH in EtOAc) to yield the intermediate acetamide (0.032 g, 26%) as a white semisolid. This substance was immediately diluted with anhydrous MeOH (7 mL), and K_2CO_3 (0.024 g, 0.174 mmol) was added. The mixture was heated at reflux for 2 h, cooled, and concentrated. The residue was diluted with EtOAc (10 mL), and the solution was washed with H_2O/sat. aq. NaCl (3:5, 8 mL). The organic layers were washed with sat. aq. NaCl (5 mL), dried over anhydrous sodium sulfate, and concentrated. The resulting syrup was diluted in CH_2Cl_2 (5 mL), filtered to remove particulate matter, and reconcentrated. To the residue was added methanolic HCl (~1.4 M, 3 mL), the mixture was stirred at room temperature for 5 min, and ether (20 mL) was added, upon which an off-white solid (0.027 g, 20%) was collected. An analytically pure sample for assay was prepared by preparative LC-MS, using the instrument and column detailed in the General Procedures section, eluting with a gradient of 95% H_2O + 0.1% formic acid/5% MeCN + 0.1% formic acid for 5 min, to 93% H_2O in 30 min, then to 0% H_2O at 32 min. Evaporation and retreatment of the residue with methanolic HCl (1 mL) and ether (1 mL) afforded the pure compound as a white flocculent solid (0.0094 g, 7.4% from **29**): mp 288–290 °C (dec). ^{1}H NMR (500 MHz; DMSO-d_6): δ 14.20 (s, 1 H), 9.07 (s, 3 H), 8.36 (dd, J = 9.2, 0.5 Hz, 1 H), 8.22 (br s, 1 H), 7.91 (d, J = 8.1 Hz, 1 H), 7.58 (s, 1 H), 7.44–7.41 (m, 3 H), 7.32 (d, J = 8.4 Hz, 2 H), 7.07 (d, J = 9.2 Hz, 1 H), 3.28–3.14 (m, 6 H), 2.97 (t, J = 8.1 Hz, 2 H). ^{13}C NMR (126 MHz; DMSO-d_6): δ 154.4 (1 C), 142.8 (1 C), 142.4 (1 C), 136.2 (1 C), 131.4 (1 C), 130.6 (1 C), 129.1 (1 C), 128.6 (1 C), 125.8 (1 C), 119.8 (1 C), 117.0 (1 C), 113.4 (1 C), 47.40 (1 C), 47.22 (1 C), 31.7 (1 C), 30.8 (1 C); one of the aminoquinoline carbons is not visible due to line-broadening. ESIMS m/z (rel. intensity) 326 (MH^+, 30). HRMS calcd for $C_{19}H_{20}ClN_3$, 325.1346; found, 325.1353.

7-Methylquinolin-2(1*H*)-one (18a) and 5-Methylquinolin-2(1*H*)-one (18b).[37,38] Compound **17** (4.26 g, 18.0 mmol) was diluted in chlorobenzene (45 mL), and anhydrous $AlCl_3$ (12.0 g, 5.00 mmol) was added. The mixture was heated to 90 °C for 2 h, upon which the solution became black. The solution was cooled and poured into ice–H_2O (300 mL), which was extracted with EtOAc (2 × 300 mL). The organic phase was washed with H_2O (200 mL), and the aqueous layer was extracted with EtOAc (100 mL). The combined organic layers were washed with sat. aq. NaCl (200 mL) and dried over anhydrous sodium sulfate. The orange solution was filtered through Celite and concentrated to afford the mixture of products as a beige solid (2.53 g, 88%) after washing with hexanes and drying. ^{1}H NMR spectra indicated that **18a** and **18b** were present as a 70:30 mixture (consistent with prior reports[37,38]), which was used without any further purification.

2-Chloro-7-methylquinoline (19a). A mixture of **18a** and **18b** (2.53 g, 15.9 mmol) was diluted in $POCl_3$ (~35 mL), and the mixture was heated at reflux for 70 min, before the clear orange solution was cooled to room temperature and poured into ice–H_2O (300 mL) in a large beaker. The beaker was immersed in ice and cooled to 0 °C with stirring, and solid NaOH was added until the pH of the mixture was approximately 7. The resultant cloudy suspension was extracted with EtOAc (300 mL), and the organic layers were washed with H_2O (100 mL) and sat. aq. NaCl (100 mL). The organic layer was dried over anhydrous sodium sulfate and concentrated, and the residue was purified by flash column chromatography (SiO_2), eluting with a gradient of hexanes to 12% ethyl acetate in hexanes to afford orange crystals. Fractional crystallization from hot isopropanol yielded pure **19a** (0.850 g, 30%) as light orange iridescent crystals; the analytical data for this compound are identical to those in prior literature reports.[39,40] ^{1}H NMR (500 MHz; $CDCl_3$): δ 8.05 (d, J = 8.5 Hz, 1 H), 8.00 (m, 1 H), 7.71 (d, J = 8.3 Hz, 1 H), 7.39 (dd, J = 8.3, 1.5 Hz, 1 H), 7.32 (d, J = 8.5 Hz, 1 H), 2.56 (s, 3 H).

2-(Acetamido)-7-methylquinoline (20). Chloride **19a** (0.300 g, 1.69 mmol) was diluted with molten anhydrous acetamide (8 g, 135 mmol), and K_2CO_3 (1.17 g, 8.45 mmol) was added. The mixture was heated in a sand bath, at reflux (~230 °C) for 17 h. The mixture was cooled, poured into H_2O (120 mL), and extracted with EtOAc (4 × 30 mL). The organic layers were washed with H_2O (3 × 100 mL) and sat. aq. NaCl (50 mL), dried over anhydrous sodium sulfate, and concentrated. Purification of the residue by flash column chromatography (SiO_2, 15% EtOAc in CH_2Cl_2) afforded the desired compound as a white solid (0.265 g, 78%). ^{1}H NMR chemical shifts for this compound are consistent with those reported by Inglis et al. for the 7-isomer.[40] ^{1}H NMR (500 MHz; $CDCl_3$): δ 9.89–9.88 (br s, 1 H), 8.40 (d, J = 8.9 Hz, 1 H), 8.15 (d, J = 9.0 Hz, 1 H), 7.67 (d, J = 8.3 Hz, 1 H), 7.58 (d, J = 0.6 Hz, 1 H), 7.29 (dd, J = 8.3, 1.4 Hz, 1 H), 2.54 (s, 3 H), 2.27 (s, 3 H).

2-(Acetamido)-7-(bromomethyl)quinoline (21). Compound **20** (0.265 g, 1.32 mmol) was diluted in anhydrous benzene (10 mL). *N*-Bromosuccinimide (0.247 g, 1.39 mmol) and a catalytic amount (~0.020 g) of benzoyl peroxide were added, and the mixture was heated to reflux under argon until an orange tint was no longer visible in the solution refluxing in the condenser (typically 4 h). The mixture was cooled, concentrated, and purified by flash column chromatography (SiO_2), eluting with a gradient of 7% to 14% EtOAc in CH_2Cl_2, to yield the product (0.236 g, 64%) as a flocculent yellow solid. ^{1}H NMR chemical shifts for this compound are consistent with those reported by Inglis et al. for the 7-isomer.[40] ^{1}H NMR (500 MHz; $CDCl_3$): δ 8.43–8.41 (m, 2 H), 8.16 (d, J = 8.9 Hz, 1 H), 7.79–7.77 (m, 2 H), 7.49 (dd, J = 8.4, 1.7 Hz, 1 H), 4.65 (s, 2 H), 2.27 (s, 3 H).

3-Fluorophenethyl Cyanide (24). 3-Fluorophenethyl bromide (**23**, 1.00 g, 12.3 mmol) was diluted in dry DMF (25 mL). Sodium cyanide (1.06 g, 61.6 mmol) was added in one portion, and the mixture was heated to 60 °C under argon for 16 h. The mixture was cooled and concentrated, and the residue was partitioned between EtOAc and H_2O (50 mL each). The layers were separated, and the aqueous phase was extracted with EtOAc (2 × 20 mL). The organic layers were washed with H_2O and sat. aq. NaCl (50 mL each), dried over anhydrous sodium sulfate, and concentrated. The resulting oil was purified by flash column chromatography (SiO_2), eluting with a gradient of 5% EtOAc in hexanes to 30% EtOAc in hexanes to yield the desired product as a colorless oil (0.638 g, 87%). ^{1}H NMR (500 MHz; $CDCl_3$): δ 7.31 (td, J = 7.9, 6.0 Hz, 1 H), 7.03–6.93 (m, 3 H), 2.96 (t, J = 7.4 Hz, 2 H), 2.63 (t, J = 7.4 Hz, 2 H).

3-(3-Fluorophenyl)-propan-1-amine (25). Compound **24** (0.180 g, 1.21 mmol) was diluted in EtOH (3 mL), and methanolic ammonia (7 M, 6 mL) and Raney nickel (~1 g) were added. The mixture was degassed and hydrogenated with a H_2-filled balloon for 30 min. The mixture was filtered through a Pall 0.2 μm syringe filter and concentrated to yield a sticky green syrup (0.083 g, 45%). The presence of amine was confirmed by ^{1}H NMR spectrometry, TLC, and ninhydrin staining, and this material was used crude without any further purification.

2-Acetamido-7-[(3-fluorophenethylamino)methyl]quinoline (26). Anhydrous Cs_2CO_3 (0.295 g, 0.906 mmol) was diluted in anhydrous DMF (10 mL). 3-Fluorophenethylamine (**22**, 0.126 g, 0.906 mmol) was added, and the mixture was stirred at room temperature for 30 min before a solution of **21** (0.220 g, 0.788 mmol) in DMF (4 mL) was added slowly over 5 min. The cloudy yellow mixture was stirred at room temperature for 16 h and concentrated. The residue was diluted with EtOAc (50 mL) and washed with H_2O (2 × 50 mL) and sat. aq. NaCl (50 mL). The organic phase was dried over anhydrous sodium sulfate, concentrated, and purified by flash column chromatography (SiO_2) eluting with 10% MeOH in EtOAc to yield the product as a clear yellow oil (0.187 g, 70%). ^{1}H NMR (500 MHz; $CDCl_3$): δ 8.95 (s, 1 H), 8.40 (br d, J = 8.2 Hz, 1 H), 8.15 (d, J = 8.9 Hz, 1 H), 7.74 (d, J = 8.3 Hz, 1 H), 7.72 (s, 1 H), 7.41 (dd, J = 8.3, 1.5 Hz, 1 H), 7.26–7.22 (m, 1 H), 6.98 (d, J = 7.7 Hz, 1 H), 6.93–6.88 (m, 2 H), 4.00 (s, 2 H), 2.95 (t, J = 7.0 Hz, 2 H), 2.85 (t, J = 7.0 Hz, 2 H), 2.23 (s, 3 H). ^{13}C NMR (126 MHz; $CDCl_3$): δ 169.3 (1 C), (163.9 + 162.0, 1 C), 151.3 (1 C), 146.5 (1 C), (142.47 + 142.41, 1 C), 142.37 (1 C), 138.5 (1C), (129.95 + 129.88, 1 C), 127.8 (1 C), 125.76 (1 C), 125.71 (1 C), 125.4 (1 C), (124.42 + 124.40, 1 C), (115.63 + 115.46, 1 C), 114.0 (1 C), (113.23 + 113.06, 1 C), 53.7 (1 C), 50.1 (1 C), 36.1 (1 C), 24.9 (1 C). ESIMS m/z (rel. intensity) 338 (MH^+, 80).

dx.doi.org/10.1021/jm401838x | J. Med. Chem. 2014, 57, 1513–1530

2-(Acetamido)-7-(cyanomethyl)quinoline (28). Compound **21** (0.216 g, 0.773 mmol) was diluted with anhydrous DMF (10 mL), and NaCN (0.190 g, 3.87 mmol) was added. The orange mixture was stirred at room temperature for 17 h. The mixture was concentrated and partitioned between EtOAc and H_2O (50 mL each), and the layers were separated. The aqueous phase was extracted with EtOAc (2 × 50 mL), and the combined organic layers were washed with H_2O (2 × 80 mL) and sat. aq. NaCl (50 mL) and dried over anhydrous sodium sulfate and concentrated. The residue was purified by flash column chromatography (SiO_2), eluting with a gradient of 15% EtOAc in CH_2Cl_2 to 25% EtOAc in CH_2Cl_2 to yield the title compound as a white solid (0.109 g, 63%): mp 180−182 °C. ^{1}H NMR (500 MHz; $CDCl_3$): δ 8.44 (dd, J = 8.3, 0.4 Hz, 1 H), 8.27−8.22 (m, 1 H), 8.18 (d, J = 9.0 Hz, 1 H), 7.81 (d, J = 8.4 Hz, 1 H), 7.79 (s, 1 H), 7.40 (dd, J = 8.3, 1.7 Hz, 1 H), 3.94 (s, 2 H), 2.28 (s, 3 H). ^{13}C NMR (126 MHz; $CDCl_3$): δ 169.2 (1 C), 151.5 (1 C), 138.8 (1 C), 132.1 (1 C), 128.7 (1 C), 126.2 (1 C), 125.6 (1 C), 124.9 (1 C), 117.3 (1 C), 114.7 (1 C), 25.1 (1 C), 24.0 (1 C). ESIMS m/z (rel. intensity) 473 (2M +Na^+, 100).

2-(Acetamido)-7-[2-aminoethyl)]quinoline (29). Compound **28** (0.060 g, 0.266 mmol) was diluted in absolute EtOH (7 mL), and methanolic ammonia (7 N, 7 mL) was added. Raney nickel (∼1.5 g, washed with H_2O and MeOH) was added, and the mixture was degassed and hydrogenated with a H_2-filled balloon at room temperature for 30 min while stirring rapidly. The clear solution was decanted from the nickel and was filtered through a Pall 0.2 μm syringe filter to remove fine particulate matter. The solution was concentrated and dried in vacuo to yield an off-white semisolid (0.062 g, 100%). Conversion to this amine was confirmed by TLC and ninhydrin staining, and it was used without any further characterization or purification.

3-Chlorophenylacetaldehyde (37).[36] Dess-Martin periodinane (1.02 g, 2.4 mmol) was diluted in anhydrous CH_2Cl_2 (25 mL) under argon, and when solution was affected, 3-chlorophenethyl alcohol (**33**, 0.313 g, 2.00 mmol) was added dropwise. The mixture was stirred for 2 h and 15 min at room temperature and was then quenched by the addition of 20 mL of sat. aq. $Na_2S_2O_3$. After stirring at room temperature for 15 min, the layers were separated, and the aqueous layer was extracted with CH_2Cl_2 (2 × 50 mL). The organic layer was washed with H_2O and sat. aq. NaCl (50 mL each) and was dried over anhydrous sodium sulfate and concentrated. The resulting semisolid residue was triturated with 10% EtOAc in hexanes, and the solid was filtered out and discarded. The filtrate was concentrated, and the oily residue was purified by flash column chromatography (SiO_2), eluting with a gradient of hexanes to 10% EtOAc in hexanes to afford the title compound as a clear yellow volatile oil (0.241 g, 78%). ^{1}H NMR (500 MHz; $CDCl_3$): δ 9.75 (t, J = 2.1 Hz, 1 H), 7.31−7.23 (m, 3 H), 7.11−7.09 (m, 1 H), 3.69 (d, J = 2.1 Hz, 2 H).

4-Chlorophenylacetaldehyde (38).[36] Dess-Martin periodinane (1.02 g, 2.4 mmol) was diluted in anhydrous CH_2Cl_2 (25 mL) under argon, and when the solution was affected, 4-chlorophenethyl alcohol (**33**, 0.313 g, 2 mmol) was added dropwise. The mixture was stirred for 2 h and 15 min at room temperature and was then quenched by the addition of 20 mL of sat. aq. $Na_2S_2O_3$. After stirring at room temperature for 15 min, the layers were separated, and the aqueous layer was extracted with CH_2Cl_2 (2 × 50 mL). The organic layer was washed with H_2O and sat. aq. NaCl (50 mL each) and was dried over anhydrous sodium sulfate and concentrated. The resulting semisolid residue was triturated with 10% EtOAc in hexanes, and the solid was filtered and discarded. The filtrate was concentrated, and the oily residue was purified by flash column chromatography (SiO_2), eluting with a gradient of hexanes to 15% EtOAc in hexanes to afford the title compound as a clear yellow volatile oil (0.211 g, 88%). ^{1}H NMR (500 MHz; $CDCl_3$): δ 9.75 (t, J = 2.1 Hz, 1 H), 7.34 (d, J = 8.3 Hz, 2 H), 7.15 (d, J = 8.2 Hz, 2 H), 3.69 (d, J = 2.0 Hz, 2 H).

3-Fluorophenyl-1-propanol (40).[44] 3-Fluorophenylpropionic acid (**39**, 0.500 g, 2.97 mmol) was diluted in anhydrous THF (2 mL) under argon and cooled to 0 °C. Borane-THF (1 M, 4.16 mL, 4.16 mmol) was added dropwise, and the mixture was allowed to warm to room temperature and stirred for 18 h. The reaction was quenched by the addition of 1:1 THF/H_2O (5 mL). When gas evolution ceased, solid K_2CO_3 was added until the mixture separated into two layers, which were separated. The aqueous layer was extracted with EtOAc (2 × 5 mL), and the combined organic layers were washed with H_2O (15 mL) and sat. aq. NaCl (15 mL), dried over anhydrous sodium sulfate, and concentrated to yield the product as a clear oil (0.446 g, 97%) after drying in vacuo. ^{1}H NMR (500 MHz; $CDCl_3$): δ 7.29−7.25 (m, 1 H), 7.00 (d, J = 7.6 Hz, 1 H), 6.95−6.89 (m, 2 H), 3.71 (t, J = 6.4 Hz, 2 H), 2.74 (t, J = 7.7 Hz, 2 H), 1.95−1.89 (m, 2 H), 1.39 (s, 1 H).

3-Fluorophenyl-1-propanal (41).[44] Anhydrous CH_2Cl_2 (10 mL) was cooled to −78 °C, and anhydrous DMSO (0.546 g, 7.00 mmol) was added, followed, dropwise, by oxalyl chloride (0.380 g, 3.00 mmol). Once gas evolution ceased, compound **40** (0.308 g, 2 mmol) was added dropwise, and the resulting milky solution was stirred for 15 min. Et_3N (1.17 mL, 8.4 mmol) was added slowly, and the mixture was stirred for 15 min at −78 °C and then warmed to room temperature and stirred for 1 h. The yellow mixture was diluted with H_2O (30 mL), and the layers were separated. The aqueous layer was extracted with CH_2Cl_2 (2 × 15 mL), and the organic layers were washed with H_2O and sat. aq. NaCl (15 mL each). The solution was dried over anhydrous sodium sulfate, concentrated, and the resulting residue was purified by flash column chromatography (SiO_2), eluting with a gradient of hexanes to 10% EtOAc in hexanes to yield the title aldehyde as a colorless volatile oil (0.220 g, 72%). ^{1}H NMR (500 MHz; $CDCl_3$): δ 9.82 (s, 1 H), 7.27−7.23 (m, 1 H), 6.97 (d, J = 7.6 Hz, 1 H), 6.92−6.89 (m, 2 H), 2.96 (t, J = 7.5 Hz, 2 H), 2.81−2.78 (m, 2 H).

2-Chloro-6-Methylquinoline (44). Compound **43** (3.75 g, 15.8 mmol) was diluted in chlorobenzene (40 mL), and aluminum chloride (10.5 g, 75.0 mmol) was added. The mixture was heated to 90 °C under nitrogen for 2 h, upon which the mixture became black, was subsequently cooled, and poured into ice−H_2O (300 g). The resulting suspension was extracted with EtOAc (700 mL), and the organic layer was washed with H_2O (300 mL) and dried over anhydrous sodium sulfate. Concentration afforded an orange solid that was recrystallized from hot MeOH (60 mL) to yield an orange iridescent solid (1.95 g, 77%). This was not characterized but was instead diluted in $POCl_3$ (30 mL) and heated at reflux for 70 min before cooling and pouring into ice−H_2O (400 mL) in a large beaker. The beaker was immersed in a cooler of ice, with stirring, and solid NaOH was added until the pH was approximately 7. The oily suspension was extracted with EtOAc (400 mL), washed with sat. aq. NaCl (300 mL), and the organic layer was dried over anhydrous sodium sulfate. The solution was concentrated to yield a solid that was purified by flash column chromatography (SiO_2), eluting with a gradient of hexanes to 40% EtOAc in hexanes to yield the product as an orange crystalline solid (1.79 g, 64% from **42**). The ^{1}H NMR chemical shifts for this compound are identical to those previously reported by Inglis et al.[40] ^{1}H NMR (500 MHz; $CDCl_3$): δ 8.01 (d, J = 8.6 Hz, 1 H), 7.91 (d, J = 9.2 Hz, 1 H), 7.57−7.55 (m, 2 H), 7.34 (d, J = 8.6 Hz, 1 H), 2.53 (s, 3 H).

2-(Acetamido)-6-methylquinoline (45). Chloride **44** (0.300 g, 1.69 mmol) was diluted with molten anhydrous acetamide (8 g, 135 mmol), and K_2CO_3 (1.17 g, 8.45 mmol) was added. The mixture was heated in a sand bath, at reflux (∼230 °C) for 16 h. The mixture was cooled, poured into H_2O (120 mL), and extracted with EtOAc (4 × 30 mL). The organic layers were washed with H_2O (3 × 100 mL) and sat. aq. NaCl (50 mL) and dried over anhydrous sodium sulfate and concentrated. Purification of the residue by flash column chromatography (SiO_2), eluting with a gradient of 10% EtOAc in CH_2Cl_2 to 30% EtOAc in CH_2Cl_2, afforded the desired compound as a white solid (0.250 g, 74%). ^{1}H NMR chemical shifts for this compound are consistent with those reported by Inglis et al.[40] ^{1}H NMR (500 MHz; $CDCl_3$): δ 8.36 (br d, J = 8.6 Hz, 1 H), 8.27 (br s, 1 H), 8.09 (d, J = 8.9 Hz, 1 H), 7.70 (d, J = 8.6 Hz, 1 H), 7.55 (s, 1 H), 7.50 (dd, J = 8.6, 1.9 Hz, 1 H), 2.51 (s, 3 H), 2.24 (s, 3 H).

2-(Acetamido)-6-(bromomethyl)quinoline (46). Compound **45** (0.300 g, 1.50 mmol) was diluted in anhydrous benzene (10 mL). *N*-Bromosuccinimide (0.280 g, 1.57 mmol) and a catalytic

amount (~0.020 g) of benzoyl peroxide were added, and the mixture was heated to reflux under nitrogen until an orange tint was no longer visible in the solution refluxing in the condenser (around 2 h 40 min). The mixture was cooled, concentrated, and purified by flash column chromatography (SiO_2), eluting with a gradient of 10% to 12% EtOAc in CH_2Cl_2 to yield the product (0.262 g, 63%) as a flocculent yellow solid. The ^{1}H NMR chemical shifts for this compound are identical to those previously reported by Inglis et al.[40] ^{1}H NMR (500 MHz; $CDCl_3$): δ 8.44 (br d, J = 8.6 Hz, 1 H), 8.30 (br s, 1 H), 8.17 (d, J = 9.0 Hz, 1 H), 7.82 (m, J = 9.1 Hz, 2 H), 7.72 (dd, J = 8.6, 2.1 Hz, 1 H), 4.67 (s, 2 H), 2.29 (s, 3 H).

2-(Acetamido)-6-(cyanomethyl)quinoline (47). Compound **46** (0.254 g, 0.91 mmol) was diluted with anhydrous DMF (10 mL), and NaCN (0.230 g, 4.55 mmol) was added. The orange mixture was stirred at room temperature for 17 h. The mixture was concentrated and partitioned between EtOAc and H_2O (50 mL each), and the layers were separated. The aqueous phase was extracted with EtOAc (2 × 50 mL), and the combined organic layers were washed with H_2O (2 × 80 mL) and sat. aq. NaCl (50 mL) and dried over anhydrous sodium sulfate and concentrated. The residue was purified by flash column chromatography (SiO_2), eluting with a gradient of 15% EtOAc in CH_2Cl_2 to 25% EtOAc in CH_2Cl_2 to yield the title compound as a white solid (0.170 g, 83%): mp 154−155 °C. ^{1}H NMR (500 MHz; $CDCl_3$): δ 8.48 (d, J = 8.6 Hz, 1 H), 8.22 (br s, 1 H), 8.20 (d, J = 9.0 Hz, 1 H), 7.85 (d, J = 8.7 Hz, 1 H), 7.81 (d, J = 1.0 Hz, 1 H), 7.61 (dd, J = 8.7, 2.1 Hz, 1 H), 3.96 (s, 2 H), 2.30 (s, 3 H). ^{13}C NMR (126 MHz; $CDCl_3$): δ 169.1 (1 C), 151.3 (1 C), 145.8 (1 C), 138.6 (1 C), 129.8 (1 C), 128.3 (1 C), 126.74 (1 C), 126.64 (1 C), 126.2 (1 C), 117.6 (1 C), 114.9 (1 C), 25.0 (1 C), 23.7 (1 C). ESIMS m/z (rel. intensity) 472 ($2M+Na^+$, 100).

2-(Acetamido)-6-(2-aminoethyl)quinoline (48). Compound **47** (0.060 g, 0.266 mmol) was diluted in absolute EtOH (7 mL), and methanolic ammonia (7 N, 7 mL) was added. Raney nickel (~1.5 g, washed with H_2O and MeOH) was added, and the mixture was degassed and hydrogenated with a balloon at room temperature for 30 min while stirring rapidly. The clear solution was decanted away from the nickel and was filtered through a Pall 0.2 μm syringe filter to remove fine particulate matter. The solution was concentrated and dried in vacuo to yield a colorless gum that became a white semisolid upon standing (0.050 g, 82%). Conversion to this amine was confirmed by ^{1}H NMR spectrometry, TLC, MS, and ninhydrin staining, and it was used crude without any further characterization or purification.

Purified NOS Enzyme Assays. Rat and human nNOS, murine macrophage iNOS, and bovine eNOS were recombinant enzymes, expressed in *E. coli* and purified as previously reported.[45,46,55−57] To test for enzyme inhibition, the hemoglobin capture assay was used to measure nitric oxide production. The assay was performed at 37 °C in HEPES buffer (100 mM, with 10% glycerol, pH 7.4) in the presence of 10 μM L-arginine. Also included were 100 μM NADPH, 0.83 mM $CaCl_2$, approximately 320 units/mL of calmodulin, 10 μM tetrahydrobiopterin, and human oxyhemoglobin (3 μM). For iNOS, $CaCl_2$ and calmodulin were omitted and replaced with HEPES buffer (as neither are required for activation of iNOS). This assay was performed in 96-well plates using a Synergy 4 BioTek hybrid reader, and the dispensing of NOS enzyme and hemoglobin were automated; after 30 s (maximum delay), NO production was read by monitoring the absorbance at 401 nm (resulting from the conversion of oxyhemoglobin to methemoglobin). Kinetic readouts were performed for 3 or 5 min. Each compound was assayed at least in duplicate, and nine concentrations (500 μM−50 nM or 100 μM−10 nM for eNOS and iNOS; 50 μM to 5 nM for nNOS) were used to construct dose−response curves. IC_{50} values were calculated by nonlinear regression using GraphPad Prism software (standard error values reported are from the $LogIC_{50}$ calculations), and K_i values were obtained using the Cheng−Prusoff equation $[K_i = IC_{50}/(1 + [S]/K_m)]$[58] using the following K_m values: 1.3 (rat nNOS), 1.6 (human nNOS), 8.2 (murine macrophage iNOS), and 1.7 μM (bovine eNOS).

Inhibitor Complex Crystal Preparation. The nNOS or eNOS heme domain proteins used for crystallographic studies were produced by limited trypsin digest from the corresponding full length enzymes and further purified through a Superdex 200 gel filtration column (GE Healthcare) as described previously.[59,60] The nNOS heme domain (at 9 mg/mL containing 20 mM histidine) or the eNOS heme domain (at 12 mg/mL containing 2 mM imidazole) was used for the sitting drop vapor diffusion crystallization setup under conditions previously reported.[59,60] Fresh crystals (1−2 days old) were first passed stepwise through cryoprotectant solutions and then soaked with a 10 mM inhibitor for 4−6 h at 4 °C before being flash cooled with liquid nitrogen.

X-ray Diffraction Data Collection, Data Processing, and Structural Refinement. The cryogenic (100 K) X-ray diffraction data were collected remotely at the Stanford Synchrotron Radiation Lightsource (SSRL) or Advanced Light Source (ALS) through the data collection control software Blu-Ice[61] and a crystal mounting robot. When a Q315r CCD detector was used, 90−100° of data were typically collected with 0.5° per frame. If a Pilatus pixel array detector was used, 120−130° of fine-sliced data were collected with 0.2° per frame. Raw CCD data frames were indexed, integrated, and scaled using HKL2000,[62] but the pixel array data were processed with XDS[63] and scaled with Scala.[64] The binding of inhibitors was detected by the initial difference Fourier maps calculated with REFMAC.[65] The inhibitor molecules were then modeled in COOT[66] and refined using REFMAC. Disordering in portions of inhibitors bound in the NOS active sites was often observed, sometimes resulting in poor density quality. However, partial structural features usually could still be visible if the contour level of the sigmaA weighted $2m|F_o| - D|F_c|$ map dropped to 0.5 σ, which afforded the building of reasonable models into the disordered regions. Water molecules were added in REFMAC and checked by COOT. The TLS[67] protocol was implemented in the final stage of refinements with each subunit as one TLS group. The omit $F_o - F_c$ density maps were calculated by repeating the last round of TLS refinement with the inhibitor coordinate removed from the input PDB file to generate the map coefficients DELFWT and PHDELWT. The refined structures were validated in COOT before deposition in the RCSB protein data bank. The crystallographic data collection and structure refinement statistics are summarized in Table S1 of the Supporting Information, with the PDB accession codes included.

Caco-2 Permeability Assay. Caco-2 monolayer assays were performed by Apredica, Inc. (Watertown, MA) using the following standard procedure: Caco-2 cells, grown in tissue culture flasks, were trypsinized, resuspended, and grown and differentiated in 96-well plates for three weeks; monolayer formation was determined by measuring transport of Lucifer yellow, an impermeable dye. All assays were performed at a concentration of 10 μM for 2 h. For apical to basolateral (A→B) permeability, compounds were added on the apical side (A), with permeation determined at the receiving (basolateral, B) side, where the receiving buffer was removed for analysis by LC/MS/MS using an Agilent 6410 mass spectrometer (ESI, MRM mode) coupled with an Agilent 1200 HPLC. Buffers used were 100 μM Lucifer yellow in transport buffer (1.98 g/L glucose in 10 mM HEPES, 1× Hank's balanced salt solution, pH 6.5) (apical side) and tranport buffer, pH 7.4 (basolateral side). Apparent permeability (P_{app}) is expressed using the following equation: $P_{app} = (dQ/dt)/C_0A$, where the numerator is the rate of permeation, C_0 is initial concentration, and A is the monolayer area. For bidirectional permeability, the efflux ratio was defined as P_{app} (B→A)/P_{app} (A→B); high efflux ratio values (>3) indicate that a compound may be a substrate for P-gp or other active transport systems.

■ ASSOCIATED CONTENT

Supporting Information

Crystallographic data collection and refinement statistics for nNOS and eNOS crystal structures containing inhibitors **5**−**9** and **15** (PDB codes 4CAM, 4CAN, 4CDT, 4CAO, 4CAP, 4CAQ, 4CAR, and 4CFT). This material is available free of charge via the Internet at http://pubs.acs.org.

AUTHOR INFORMATION

Corresponding Authors

*(T.L.P.) Tel:+1 949 824 7020. E-mail: poulos@uci.edu.
*(R.B.S.) Tel:+1 847 491 5653. Fax: +1 847 491 7713. E-mail: Agman@chem.northwestern.edu.

Notes

The authors declare no competing financial interest.

ACKNOWLEDGMENTS

We are grateful to the Baxter-Northwestern University Alliance, (to R.B.S.), and to the National Institutes of Health (GM049725, to R.B.S.; GM057353 to T.L.P.), for support of this work. We thank Dr. Bettie Sue Masters (NIH Grant GM52419, with whose laboratory P.M. and L.J.R. are affiliated). Additional support was provided by the Robert A. Welch Foundation to Dr. Bettie Sue Masters (AQ1192). P.M. is supported by grants 0021620806 and 1M0520 from MSMT of the Czech Republic. M.A.C. wishes to thank Dr. Zhidong Ma and Ms. Kasia Catherman of the Center for Molecular Innovation and Drug Discovery (Northwestern University) for valuable assistance with preparative HPLC, and Mr. Saman Shafaie and Mr. Daniel Sweeney for assistance with HRMS experiments. H.L. thanks Mariko Ogura for assistance in structure refinements. We also thank the SSRL and ALS beamline staff for their support during X-ray diffraction and data collection.

ABBREVIATIONS USED

nNOS, neuronal nitric oxide synthase; iNOS, inducible nitric oxide synthase; eNOS, endothelial nitric oxide synthase; FMN, flavin mononucleotide; H_4B, (6*R*)-5,6,7,8-tetrahydrobiopterin; tPSA, total polar surface area; P_{app}, apparent permeability; HEPES, 4-(2-hydroxyethyl)-1-piperazineethanesulfonic acid

REFERENCES

(1) Knowles, R. G.; Moncada, S. Nitric oxide synthases in mammals. *Biochem. J.* **1994**, *298*, 249−258.

(2) Uehara, T.; Nakamura, T.; Yao, D.; Shi, Z. Q.; Gu, Z.; Ma, Y.; Masliah, E.; Nomura, Y.; Lipton, S. A. S-Nitrosylated protein-disulphide isomerase links protein misfolding to neurodegeneration. *Nature* **2006**, *441*, 513−517.

(3) Torreilles, F.; Salman-Tabcheh, S.; Guerin, M.; Torreilles, J. Neurodegenerative disorders: the role of peroxynitrite. *Brain Res. Brain Res. Rev.* **1999**, *30*, 153−163.

(4) Zhang, L.; Dawson, V. L.; Dawson, T. M. Role of nitric oxide in Parkinson's disease. *Pharmacol. Ther.* **2006**, *109*, 33−41.

(5) Dorheim, M.-A.; Tracey, W. R.; Pollock, J. S.; Grammas, P. Nitric oxide synthase activity is elevated in brain microvessels in Alzheimer's disease. *Biochem. Biophys. Res. Commun.* **1994**, *205*, 659−665.

(6) Norris, P. J.; Waldvogel, H. J.; Faull, R. L. M.; Love, D. R.; Emson, P. C. Decreased neuronal nitric oxide synthase messenger RNA and somatostatin messenger RNA in the striatum of Huntington's disease. *Neuroscience* **1996**, *72*, 1037−1047.

(7) Dreschel, D. A.; Estevez, A. G.; Barbeito, L.; Beckman, J. S. Nitric oxide-mediated oxidative damage and the progressive demise of motor neurons in ALS. *Neurotox. Res.* **2012**, *22*, 251−264.

(8) Huang, Z.; Huang, P. L.; Panahian, N.; Dalkara, T.; Fishman, M. C.; Moskowitz, M. A. Effects of cerebral ischemia in mice deficient in neuronal nitric oxide synthase. *Science* **1994**, *265*, 1883−1885.

(9) Dawson, V. L.; Dawson, T. M.; Uhl, G. R.; Snyder, S. H. Human immunodeficiency virus type 1 coat protein neurotoxicity mediated by nitric oxide in primary cortical cultures. *Proc. Natl. Acad. Sci. U.S.A.* **1993**, *90*, 3256−3259.

(10) Ramachandran, R.; Ploug, K. B.; Hay-Schmidt, A.; Oleson, J.; Janson-Oleson, J.; Gupta, S. Nitric oxide synthase (NOS) in the trigeminal vascular system and other brain structures related to pain in rats. *Neurosci. Lett.* **2010**, *484*, 192−196.

(11) Matter, H.; Kotsonis, P. Biology and chemistry of the inhibition of nitric oxide synthases by pteridine-derivatives as therapeutic agents. *Med. Res. Rev.* **2004**, *24*, 662−684.

(12) Masic, L. P. Arginine mimetic structures in biologically active antagonists and inhibitors. *Curr. Med. Chem.* **2006**, *13*, 3627−3648.

(13) Hobbs, A. J.; Higgs, A.; Moncada, S. Inhibition of nitric oxide synthase as a potential therapeutic target. *Annu. Rev. Pharmacol.* **1999**, *39*, 191−220.

(14) Siddhanta, U.; Presta, A.; Fan, B.; Wolan, D.; Rousseau, D. L.; Stuehr, D. J. Domain swapping in inducible NO synthase: electron transfer occurs between flavin and heme groups located on adjacent subunits in the dimer. *J. Biol. Chem.* **1998**, *273*, 18950−18958.

(15) Rosen, G. M.; Tsai, P.; Pou, S. Mechanism of free-radical generation by nitric oxide synthase. *Chem. Rev.* **2002**, *102*, 1191−1199.

(16) Alderton, W. K.; Cooper, C. E.; Knowles, R. G. Nitric oxide synthases: structure, function and inhibition. *Biochem. J.* **2001**, *357*, 593−615.

(17) Ji, H.; Stanton, B. Z.; Igarashi, J.; Li, H.; Martásek, P.; Roman, L. J.; Poulos, T. L.; Silverman, R. B. Minimal pharmacophoric elements and fragment hopping, an approach directed at molecular diversity and isozyme selectivity. Design of selective neuronal nitric oxide synthase inhibitors. *J. Am. Chem. Soc.* **2008**, *130*, 3900−3914.

(18) Ji, H.; Delker, S. L.; Li, H.; Martásek, P.; Roman, L. J.; Poulos, T. L.; Silverman, R. B. Exploration of the active site of neuronal nitric oxide synthase by the design and synthesis of pyrrolidinomethyl 2-aminopyridine derivatives. *J. Med. Chem.* **2010**, *53*, 7804−7824.

(19) Ji, H.; Tan, S.; Igarashi, J.; Li, H.; Derrick, M.; Martásek, P.; Roman, L. J.; Vasquez-Vivar, J.; Poulos, T. L.; Silverman, R. B. Selective neuronal nitric oxide synthase inhibitors and the prevention of cerebral palsy. *Ann. Neurol.* **2009**, *65*, 209−217.

(20) Veber, D. F.; Johnson, S. R.; Cheng, H.-Y.; Smith, B. R.; Ward, H. W.; Kopple, K. D. Molecular properties that influence the oral bioavailability of drug candidates. *J. Med. Chem.* **2002**, *35*, 2615−2623.

(21) Seelig, A. The role of size and charge for blood-brain barrier permeation of drugs and fatty acids. *J. Mol. Neurosci.* **2007**, *33*, 32−41.

(22) Li, H.; Xue, F.; Kraus, J. M., II; Ji, H.; Jansen Labby, K.; Mataka, J.; Delker, S. L.; Martásek, P.; Roman, L. J.; Poulos, T. L.; Silverman, R. B. Cyclopropyl- and methyl-containing inhibitors of neuronal nitric oxide synthase. *Bioorg. Med. Chem.* **2013**, *21*, 1333−1343.

(23) Xue, F.; Fang, J.; Lewis, W. W.; Martásek, P.; Roman, L. J.; Silverman, R. B. Potent and selective neuronal nitric oxide synthase inhibitors with improved cellular permeability. *Bioorg. Med. Chem. Lett.* **2010**, *15*, 554−557.

(24) Xue, F.; Huang, J.; Ji, H.; Fang, J.; Li, H.; Martásek, P.; Roman, L. J.; Poulos, T. L.; Silverman, R. B. Structure-based design, synthesis, and biological evaluation of lipophilic-tailed monocationic inhibitors of neuronal nitric oxide synthase. *Bioorg. Med. Chem.* **2010**, *18*, 6526−6537.

(25) Lawton, G. R.; Ranaivo, H. R.; Chico, L. K.; Ji, H.; Xue, F.; Martásek, P.; Roman, L. J.; Watterson, D. M.; Silverman, R. B. Analogues of 2-aminopyridine-based selective inhibitors of neuronal nitric oxide synthase with increased bioavailability. *Bioorg. Med. Chem.* **2009**, *17*, 2371−2380.

(26) Huang, H.; Li, H.; Yang, S.; Chreifi, G.; Martásek, P.; Roman. L. J.; Meyskens, F. L.; Poulos, T. L.; Silverman, R. B. Potent and selective double-headed thiophene-2-carboximidamide inhibitors of neuronal nitric oxide synthase for the treatment of melanoma, unpublished work.

(27) Fedorov, R.; Vasan, R.; Ghosh, D. K.; Schlichting, I. Structures of nitric oxide synthase isoforms complexed with the inhibitor AR-R17477 suggest a rational basis for specificity and inhibitor design. *Proc. Nat. Acad. Sci. U.S.A.* **2004**, *101*, 5892−5897.

(28) Fang, J.; Silverman, R. B. A cellular model for screening neuronal nitric oxide synthase inhibitors. *Anal. Biochem.* **2009**, *390*, 74−78.

(29) Dewick, P. M. *Essentials of Organic Chemistry For Students of Pharmacy, Medicinal Chemistry, and Biological Chemistry*; John Wiley and Sons, Ltd., West Sussex, U.K., 2006; p 441.
(30) Paudler, W. W.; Blewitt, H. L. Ten π electron nitrogen heterocyclic compounds. V. The site of protonation and *N*-methylation of imidazo[1,2-α] pyridines and the planarity of the ring system. *J. Org. Chem.* **1966**, *31*, 1295−1298.
(31) Jaroch, S.; Holscher, P.; Rehwinkel, H.; Sulzle, D.; Burton, G.; Hillmann, M.; McDonald, F. M. Dihydroquinolines as novel n-NOS inhibitors. *Bioorg. Med. Chem. Lett.* **2002**, *12*, 2561−2564.
(32) Jaroch, S.; Rehwinkel, H.; Holscher, P.; Sulzle, D.; Burton, G.; Hillmann, M.; McDonald, F. M.; Miklautz, H. Fluorinated dihydroquinolines as potent n-NOS inhibitors. *Bioorg. Med. Chem. Lett.* **2004**, *14*, 743−746.
(33) Jaroch, S.; Holscher, P.; Rehwinkel, H.; Sulzle, D.; Burton, G.; Hillmann, M.; McDonald, F. M. Dihydroquinolines with amine-containing side chains as potent n-NOS inhibitors. *Bioorg. Med. Chem. Lett.* **2003**, *13*, 1981−1984.
(34) Cheng, Y.; Judd, T. C.; Bartberger, M. D.; Brown, J.; Chen, K.; Fremeau, R. T.; Hickman, D.; Hitchcock, S. A.; Jordan, B.; Li, V.; Lopez, P.; Louie, S. W.; Luo, Y.; Michelsen, K.; Nixey, T.; Powers, T. S.; Rattan, C.; Sickmier, E. A.; St. Jean, D. J.; Wahl, R. C.; Wen, P. H.; Wood, S. From fragment screening to in vivo efficacy: optimization of a series of 2-aminoquinolines as potent inhibitors of beta-site amyloid precursor protein cleaving enzyme 1 (BACE1). *J. Med. Chem.* **2011**, *54*, 5836−5857.
(35) Xue, F.; Li, H.; Fang, J.; Roman, L. J.; Martásek, P.; Poulos, T. L.; Silverman, R. B. Peripheral but crucial: A hydrophobic pocket (Tyr706, Leu337, and Met336) for potent and selective inhibition of neuronal nitric oxide synthase. *Biooorg. Med. Chem. Lett.* **2010**, *20*, 6258−6261.
(36) Ji, H.; Li, H.; Martásek, P.; Roman, L. J.; Poulos, T. L.; Silverman, R. B. Discovery of highly potent and selective inhibitors of neuronal nitric oxide synthase by fragment hopping. *J. Med. Chem.* **2009**, *52*, 779−797.
(37) Manimaran, T.; Thiruvengadam, T. K.; Ramakrishnan, V. T. Synthesis of coumarins (2-oxo-2*H*-1-benzopyrans), thiacoumarins (2-oxo-2*H*-1-benzothiopyrans), and carbostyrils (2-oxo-1,2-dihydroquinolines). *Synthesis* **1975**, 739−741.
(38) Johnston, K. M.; Luker, R. M.; Williams, G. H. Friedel Crafts cyclisations. Synthesis of derivatives of 2(1H)-quinolone (carbostyril) by aluminum chloride-catalysed cycloeliminations of cinnamanilide and related compounds. *J. Chem. Soc. Perkin Trans. 1* **1972**, 1648−1652.
(39) Warner, P.; Barker, A. J.; Jackman, A. L.; Burrows, K. D.; Roberts, N.; Bishop, J. A. M.; O'Connor, B. M.; Hughes, L. R. Quinoline antifolate thymidylate synthase inhibitors: variation of the C2- and C4-substituents. *J. Med. Chem.* **1992**, *35*, 2761−2768.
(40) Inglis, S.; Jones, R.; Fritz, D.; Stojkoski, C.; Booker, G.; Pyke, S. Synthesis of 5-, 6- and 7-substituted-2-aminoquinolines as SH3 domain ligands. *Org. Biomol. Chem.* **2005**, *3*, 2543−2557.
(41) Hazeldine, S. T.; Polin, L.; Kushner, J.; White, K.; Bouregeois, N. M.; Crantz, B.; Palomino, E.; Corbett, T. H.; Horwitz, J. P., II. Synthesis and biological evaluation of some bioisosteres and congeners of the antitumor agent, 2-{4-[(7-chloro-2-quinoxalinyl)oxy]phenoxy}-propionic acid (XK469). *J. Med. Chem.* **2002**, *45*, 3130−3137.
(42) Kóródi, F. A simple new synthetic method for the preparation of 2-aminoquinolines. *Synth. Commun.* **1991**, *21*, 1841−1846.
(43) Salvatore, R. N.; Nagle, A. S.; Jung, K. W. Cesium effect: high chemoselectivity in direct *N*-alkylation of amines. *J. Org. Chem.* **2002**, *67*, 674−683.
(44) Batt, D. G. *N*-Substituted Heterocyclic Amines as Modulators of Chemokine Receptor Activity. WO2004/028530, Apr 8, 2004.
(45) Labby, K. J.; Xue, F.; Kraus, J. M.; Ji, H.; Mataka, J.; Li, H.; Martásek, P.; Roman, L. J.; Poulos, T. L.; Silverman, R. B. Intramolecular hydrogen bonding: A potential strategy for more bioavailable inhibitors of neuronal nitric oxide synthase. *Bioorg. Med. Chem.* **2012**, *20*, 2435−2443.
(46) Hevel, J. M.; Marletta, M. A. Nitric-oxide synthase assays. *Methods Enzymol.* **1994**, *233*, 250−258.
(47) Raman, C. S.; Li, H.; Martásek, P.; Kral, V.; Masters, B. S. S.; Poulos, T. L. Crystal structure of constitutive endothelial nitric oxide synthase: A paradigm for pterin function involving a novel metal center. *Cell* **1998**, *95*, 939−950.
(48) Hagmann, W. K.; Caldwell, C. G.; Chen, P.; Durette, P. L.; Esser, C. K.; Lanza, T. J.; Kopka, I. E.; Guthikonda, R.; Shah, S. K.; MacCoss, M.; Chabin, R. M.; Fletcher, D.; Grant, S. K.; Green, B. G.; Humes, J. L.; Kelly, T. M.; Luell, S.; Meurer, R.; Moore, V.; Pacholok, S. G.; Pavia, T.; Wolliams, H. R.; Wong, K. K. Substituted 2-aminopyridines as inhibitors of nitric oxide synthases. *Bioorg. Med. Chem. Lett.* **2000**, *10*, 1975−1978.
(49) Delker, S. L.; Ji, H.; Li, H.; Jamal, J.; Fang, J.; Xue, F.; Silverman, R. B.; Poulos, T. L. Unexpected binding modes of nitric oxide synthase inhibitors effective in the prevention of cerebral palsy. *J. Am. Chem. Soc.* **2010**, *132*, 5437−5442.
(50) Flinspach, M.; Li, H.; Jamal, J.; Yang, W.; Huang, H.; Silverman, R. B.; Poulos, T. L. Structures of the neuronal and endothelial nitric oxide synthase heme domain with D-nitroarginine-containing dipeptide inhibitors bound. *Biochemistry* **2004**, *43*, 5181−5185.
(51) Ji, H.; Gomez-Vidal, J. A.; Martásek, P.; Roman, L. J.; Silverman, R. B. Conformationally restricted dipeptide amides as potent and selective neuronal nitric oxide synthase inhibitors. *J. Med. Chem.* **2006**, *49*, 6254−6263.
(52) Ji, H.; Li, H.; Flinspach, M.; Poulos, T. L.; Silverman, R. B. Computer modeling of selective regions in the active site of nitric oxide synthases: implication for the design of isoform-selective inhibitors. *J. Med. Chem.* **2003**, *46*, 5700−5711.
(53) Lohmann, C.; Huwel, S.; Galla, H. J. Predicting blood-brain barrier permeability of drugs: evaluation of different in vitro assays. *J. Drug Targeting* **2002**, *10*, 263−276.
(54) Stewart, B. H; Chan, O. H.; Lu, R. H.; Reyner, E. L.; Shmid, H. L.; Hamilton, H. W.; Steinbaugh, B. A.; Taylor, M. D. Comparison of intestinal permeabilities determined in multiple *in vitro* and *in situ* models: relationship to absorption in humans. *Pharm. Res.* **1995**, *12*, 693−699.
(55) Roman, L. J.; Sheta, E. A.; Martásek, P.; Gross, S. S.; Liu, Q.; Masters, B. S. S. High-level expression of functional rat neuronal nitric oxide synthase in *Escherichia coli*. *Proc. Natl. Acad. Sci. U.S.A.* **1995**, *92*, 8428−8432.
(56) Hevel, J. M.; White, K. A.; Marletta, M. A purification of the inducible murine macrophage nitric oxide synthase: identification as a flavoprotein. *J. Biol. Chem.* **1991**, *266*, 22789−22791.
(57) Gerber, N. C.; Ortiz de Montellano, P. R. Neuronal nitric oxide synthase: expression in *Escherichia coli*, irreversible inhibition by phenyldiazene, and active site topology. *J. Biol. Chem.* **1995**, *270*, 17791−17796.
(58) Cheng, Y.-C.; Prusoff, W. H. Relationship between the inhibition constant (K_i) and the concentration of the inhibitor which causes 50% inhibition (IC_{50}) of an enzymatic reaction. *Biochem. Pharmacol.* **1973**, *22*, 3099−3108.
(59) Li, H.; Shimizu, H.; Flinspach, M.; Jamal, J.; Yang, W.; Xian, M.; Cai, T.; Wen, E. Z.; Jia, Q.; Wang, P. G.; Poulos, T. L. The novel binding mode of *N*-alkyl-*N*′-hydroxyguanidine to neuronal nitric oxide synthase provides mechanistic insights into NO biosynthesis. *Biochemistry* **2002**, *41*, 13868−13875.
(60) Raman, C. S.; Li, H.; Martásek, P.; Král, V.; Masters, B. B. S.; Poulos, T. L. Crystal structure of constitutive endothelial nitric oxide synthase: a paradigm for pterin function involving a novel metal center. *Cell* **1998**, *95*, 939−950.
(61) McPhillips, T. M.; McPhillips, S. E.; Chiu, H. J.; Cohen, A. E.; Deacon, A. M.; Ellis, P. J.; Garman, E.; Gonzalez, A.; Sauter, N. K.; Phizackerley, R. P.; Soltis, S. M.; Kuhn, P. Blu-Ice and the Distributed Control System: software for data acquisition and instrument control at macromolecular crystallography beamlines. *J. Synchrotron Radiat.* **2002**, *9*, 401−406.
(62) Otwinowski, Z.; Minor, W. Processing of X-ray diffraction data collected in oscillation mode. *Methods Enzymol.* **1997**, *276*, 307−326.

(63) Kabsch, W. XDS. *Acta Crystallogr., Sect. D* **2010**, *66*, 125−132.
(64) Evans, P. R. Scaling and assessment of data quality. *Acta Crystallogr., Sect. D* **2006**, *62*, 72−82.
(65) Murshudov, G. N.; Vagin, A. A.; Dodson, E. J. Refinement of macromolecular structures by the maximum-likelihood method. *Acta Crystallogr., Sect. D* **1997**, *53*, 240−255.
(66) Emsley, P.; Cowtan, K. Coot: model-building tools for molecular graphics. *Acta Crystallogr., Sect. D* **2004**, *60*, 2126−2132.
(67) Winn, M. D.; Isupov, M. N.; Murshudov, G. N. Use of TLS parameters to model anisotropic displacements in macromolecular refinement. *Acta Crystallogr., Sect. D* **2001**, *57*, 122−133.